U.PORTO

MESTRADO ONCOLOGIA

ESPECIALIDADE EM ONCOLOGIA LABORATORIAL

The role of VHL/HIF axis- dependent metabolic profile in clear cell renal cell carcinoma aggressiveness

Ana Beatriz Costa

M

2022

U.PORTO

Ana Beatriz Costa. The role of VHL/HIF axis- dependent metabolic profile in clear cell renal cell carcinoma aggressiveness

M.ICBAS.2022

The role of VHL/HIF axis- dependent metabolic profile in clear cell renal cell carcinoma aggressiveness s

Ana Beatriz Costa

INSTITUTO DE CIÊNCIAS BIOMÉDICAS ABEL SALAZAR

Ana Beatriz Ferreira Costa

The role of VHL/HIF axis- dependent metabolic profile in clear cell renal cell carcinoma aggressiveness.

Dissertação de Candidatura ao grau de Mestre em Oncologia – Especialização em Oncologia Laboratorial submetida ao Instituto de Ciências Biomédicas de Abel Salazar da Universidade do Porto

Orientadora: **Doutora Vera Miranda Gonçalves**

Investigadora Júnior no Grupo de Epigenética e Biologia do Cancro

Centro de Investigação

Instituto Português de Oncologia do Porto Francisco Gentil, E.P.E

Coorientadora: **Professora Doutora Carmen de Lurdes Fonseca Jerónimo**

Professora Catedrática Convidada

Departamento de Patologia e Imunologia Molecular

Instituto de Ciências Biomédicas Abel Salazar - Universidade do Porto

Investigadora Auxiliar, Coordenadora do Grupo de Epigenética e Biologia do Cancro,

Diretora do Centro de Investigação

Instituto Português de Oncologia do Porto Francisco Gentil, E.P.E

This study was funded by a grant of the Research Centre of Portuguese Oncology Institute of Porto (CI-IPOP-92-2018-MCTKidCan).

AGRADECIMENTOS

Quando há 3 anos me deparei com o grupo de Epigenética e Biologia do Cancro no site do IPO do Porto estava longe de imaginar o quão gratificante seriam estes últimos anos, tanto a nível pessoal como profissional. E como nada na vida se faz sozinho, não poderia deixar de agradecer a todas as pessoas que me acompanharam neste percurso.

Em primeiro lugar, à minha orientadora Doutora Vera Miranda-Gonçalves e à minha co-orientadora, Professora Doutora Carmen Jerónimo. À professora, na qualidade de Diretora do Centro de Investigação do IPO-Porto, pelo voto de confiança em realizar este projeto. Como coordenadora do GEBC, por me ter dado a oportunidade de explorar a área de oncologia quando estava a terminar a minha licenciatura que me levou a frequentar mais tarde o mestrado em Oncologia. Por todas as correções e sugestões feitas ao nosso trabalho e por me transmitir os valores da ciência. À Vera, ou melhor orientadora que se pode pedir, pela paciência e disponibilidade constantes. Por me acompanhar sempre, por atender as minhas chamadas de sábado à noite e responder às mensagens de domingo de manhã. Por todos os ensinamentos, críticas, opiniões e conselhos. A Vera ensina-me há 3 anos (praticamente) tudo o que sei de ciência e nunca vão existir palavras para expressar a minha gratidão por ter sido ela a acompanhar-me.

Aos meus 4 companheiros desta aventura, pela fotossíntese e momento zen diário. Pelas napis, torradinhas e momentos de purificação. À Margareta, pelo coração bom que ajuda toda a gente, por solucionar todos os nossos problemas no citómetro e pela experiência de vida que nos vai transmitindo nas pequenas coisas. À Bianca por nos mostrar que o mundo é pequeno e que, mesmo longe, continua a alegrar os nossos dias com o “bom diaaa o sol já nasceu aqui no abrigo”. À pipita, rainha dramática favorita, obrigada por saíres de casa às 21h para me abrires a porta do lab, por alinhares num ramenzinho nos dias em que eu estou triste e por dizeres que nós somos incríveis sempre que duvidamos disso. Ao Tiguinho, por me acompanhar nesta aventura há tanto tempo sem ainda se ter fartado de mim (e eu da má disposição matinal dele). Por me ensinar aquilo que aprende e ouvir aquilo que me ensinam. Por ser o meu melhor amigo e a pessoa mais fiel, dentro e fora do laboratório, dos dias bons e dos dias menos bons.

Ao Zé, à Sofia, à Macedo, à Teixas, ao João, à Nair e a todos os membros do GEBC por me ajudarem e transmitirem sempre o seu conhecimento. Por me terem acolhido e por todas as sugestões que foram dando ao longo deste ano, que permitiram que este trabalho fosse realizado.

À família que o Porto me deu, agradeço por terem tornado estes 5 anos os melhores da minha vida. Pelos momentos de festa, estudo intensivo e por me permitirem criar as

melhores memórias. Ao Diogo, Miguel e Tina por terem tornado o mestrado tão mais fácil. À Mon (Carolina ou Mónica), Daniela, Inês e Mafalda, por serem o cliché dos amigos para a vida. Por partilharem e continuarem a criar comigo as melhores memórias. Por me permitirem crescer e evoluir com elas e por nunca me deixarem cair. O melhor da faculdade são as pessoas e eu não escolhia outras para partilhar esta experiência.

Por fim, às pessoas de casa. Aos amigos de infância, à Raquel e à Maria em especial, por me acompanharem sempre. À minha família pelo amor, comidinha e carinho. Aos meus pais, as melhores pessoas do mundo, que me dão liberdade para ser o que quiser sem nunca duvidarem de mim. Por me incentivarem sempre a seguir aquilo que me faz feliz. Tudo o que sou devo a eles.

Chego ao fim desta etapa de coração (muito) cheio!

ABSTRACT

Background: Clear cell renal cell carcinoma (ccRCC) is the most common type of renal cell carcinomas. The Von Hippel-Lindau (VHL) tumour suppressor gene is frequently altered in ccRCC. VHL inactivation leads to hypoxia inducible factors (HIFs) accumulation and a hypoxic-related metabolic reprogramming, with glycolytic enzyme's upregulation and an increased lactate production. Lactate is transported to the tumour microenvironment through the monocarboxylate transporters 1 and 4 (MCT1 and MCT4), contributing to an increased aggressiveness and poor prognosis (however little is known about ccRCC). Our main goal is to understand the interplay between VHL inactivation and the glycolytic phenotype, particularly for MCTs expression (deregulation) in the ccRCC aggressiveness, in order to identify new therapeutic strategies.

Methods: MCTs effect on disease progression was evaluated in ccRCC cell lines (769-P, 786-O and Caki-1) with different VHL status, using the CRISPR-Cas9 technology to obtain MCT1 or MCT4 knockdown. Alterations in cell growth, proliferation, migration, and invasion were assessed through *in vitro* assays. *In vivo* studies using the chorioallantoic membrane (CAM) assay were performed in order to validate our *in vitro* findings. HIF-1α and HIF-2α expressions were evaluated by qRT-PCR in a series of human ccRCC tumours (n=200) and normal kidney tissues (n=30).

Results: HIF-1α expression was downregulated in ccRCC cases but within these, increased with tumour stage. HIF-2α was upregulated in ccRCC when compared to normal kidney. 769-P and 786-O cell lines, which lack VHL, display a higher glycolytic phenotype compared to Caki-1, which does not harbours VHL mutations. Both MCT1 and MCT4 knockdown cells showed lower tumour growth and proliferation when compared to the scramble cells. Furthermore, MCT4, but not MCT1, knockdown leads to lower rates of tumour migration and invasion. Smaller *in vivo* micro-tumours were formed in both MCT1 and MCT4 knockdown cells but lower vessel recruitment was prominent in clones with less MCT4 expression.

Conclusions: HIF-2α is important for ccRCC phenotype establishment and maintenance, whilst HIF-1α is involved in tumour progression and related to poor prognosis. MCT1 and MCT4 revealed to be important for tumour growth. However, MCT4 seems to be a key player in sustaining the aggressive phenotype, leading to the idea that different MCTs should be targeted across ccRCC disease progression.

RESUMO

Abstract: O carcinoma renal de células claras (ccRCC) é o tipo de carcinoma renal mais frequente. O gene supressor tumoral Von Hipper-Lindau (VHL) está frequentemente inativo em ccRCC. A sua inativação leva à acumulação de fatores indutores de hipoxia (HIFs) e, por conseguinte, a uma reprogramação metabólica relacionada, com consequente aumento na expressão de enzimas glicolíticas e na produção de lactato exacerbada. O lactato é transportado para o microambiente tumoral (TME) através dos transportadores de monocarboxilato 1 e 4 (MCT1 e MCT4), contribuindo para um aumento da agressividade e mau prognóstico. O nosso objetivo é perceber a interligação entre o estado inativo do VHL e o fenótipo glicolítico, particularmente a expressão de MCTs na agressividade da ccRCC, de forma a identificar novas estratégias terapêuticas.

Métodos: O efeito dos MCTs na progressão da doença foi avaliado em linhas celulares de ccRCC (769-P, 786-O e Caki-1) com diferentes status de VHL, usando a tecnologia de CRISP-Cas9 para obter uma expressão de MCTs diminuída. Alterações no crescimento, proliferação, migração e invasão celulares foram avaliados através de estudos *in vitro*. Estudos *in vivo* foram efetuados na membrana coroalontóide (CAM) do embrião de galinha para validar os resultados. As expressões de HIF-1α e HIF-2α foram avaliadas por *qRT-PCR* numa série de ccRCC humanos (n=200) e em rim normal (n=30).

Resultados: A expressão de HIF-1α encontra-se diminuída em casos de ccRCC mas, dentro destes, aumenta com o estadio tumoral. HIF-2α estava aumentado em ccRCC quando comparado com rim normal. As linhas celulares 769-P and 786-O, que não expressam VHL, têm um fenótipo glicolítico mais elevado do que a Caki-1, que expressa VHL. As células com MCT1 e MCT4 silenciados demonstraram menor crescimento tumoral do que a condição controlo. Para além disso, células silenciadas para MCT4, mas não para MCT1, apresentaram menores taxas de migração e invasão. Células com silenciamento do MCT1 ou MCT4 formaram tumores menores, mas o recrutamento de vasos foi proeminente nas células silenciadas para o MCT4 no ensaio da CAM.

Conclusões: HIF-2α é importante para estabelecer e manter o fenótipo de ccRCC mas o HIF-1α está envolvido na progressão tumoral e relacionado com mau prognóstico. Tanto o MCT1 como o MCT4 demonstraram ser importantes no crescimento tumoral. No entanto, o MCT4 parece ser importante a sustentar o fenótipo agressivo, levando a concluir que diferentes isoformas dos MCTs deveriam ser putativos alvos terapêuticos ao longo da progressão do ccRCC.

TABLE OF CONTENTS

1. INTRODUCTION 1
1.1. Kidney cancer 1
1.1.1. Epidemiology 1
1.1.2. Diagnosis and treatment 1
1.1.3. Risk factors 2
1.2. Renal cell carcinoma classification 2
1.2.1. Clear Cell Renal Cell Carcinoma 3
1.3. Epigenetic 3
1.3.1. DNA methylation 4
1.4. Tumour cell metabolism 5
1.4.1. Metabolic alterations in RCC 6
1.4.2. Metabolic reprogramming in ccRCC 8
1.5. Monocarboxylate transporters family 9
1.5.1. MCT1 and MCT4 metabolic roles in tumour cells 10
1.5.2. Lactate in tumour microenvironment 12
1.6. MCTs as therapeutic targets in cancer 13
2. PRELIMINARY RESULTS 14
3. AIMS 18
4. MATERIALS AND METHODS 19
4.1. Cell lines culture 19
4.2. Tissue samples 19
4.3. DNA extraction and quantitative polymerase chain reaction (qPCR) 19
4.4. RNA extraction, cDNA synthesis and quantitative reverse transcriptase polymerase chain reaction (Qrt-PCR) 20
4.5. MCTs knockdown: CRIPSR/Cas9 technology 21
4.6. Western blot 22
4.7. Immunofluorescence 23
4.8. Metabolism assay 24
4.9. Trypan blue dye exclusion assay 25
4.10. Colony formation assay 25
4.11. Proliferation assay 26
4.12. Invasion assay 26
4.13. Wound-healing assay 27
4.14. Chorioallantoic membrane (CAM) assay 28
4.15. Statistical analysis 28

5. RESULTS 29
5.1. VHL status characterization in ccRCC 29
5.2. HIF-2α was upregulated in ccRCC patients' samples 29
5.3. Glycolytic and hypoxia markers were differently expressed in ccRCC lines 30
5.4. MCTs downregulation affected glycolytic metabolism, decreasing the lactate production 31
5.5. MCTs knockdown altered an HIF-related glycolytic phenotype in ccRCC cells 35
5.6. MCTs inhibition' affected tumour growth and proliferation 38
5.7. MCTs inhibition' contributed to a less aggressive phenotype in ccRCC cells 40
5.8. MCTs role in *in vivo* tumour formation and progression 43
6. DISCUSSION 45
7. CONCLUSIONS 51
8. FUTURE PERSPECTIVES 52
9. REFERENCES 53

FIGURE INDEX

Figure 1. Worldwide RCC incidence and mortality distributions. 2020 global incidence (blue) and mortality (red) rates for both sexes estimated age-standardized. Via Globocan. 1

Figure 2. Epigenetic mechanisms involved in gene expression regulation. Chromatin remodelling complexes, histone variants, histone post-translational modifications and DNA methylation regulate gene transcription through chromatin structure modulation. Adapted from [21]. 4

Figure 3. DNA methylation regulation. DNMTs catalyse cytosine methylation using SAM as a methyl donor and reducing it to SAH. TETs revert DNA methylation by converting 5'Methyl-Cytosine into 5'Hydroxymethyl-Cytosine through a hydroxylation alpha-ketoglutarate dependent reaction. Gene promoter hypermethylation inhibits transcription. Abbreviations: DNMT- DNA methyltransferase; SAH- Sadenosylhomocysteine; SAM- S-adenosyl-L-methionine; TET- Ten-eleven translocation. 5

Figure 4. Hallmarks of cancer. The cancer hallmarks comprise biological mechanisms adaptations that cancer cells rewire to favoring tumour growth and aggressiveness..... 6

Figure 5. Metabolic reprogramming in RCC. Renal cell carcinomas are characterized by a high glycolytic phenotype with increased glucose uptake and lactate production. Pentose phosphate pathway, fatty acid synthesis and glutaminolysis are increased to sustain nucleotides, amino acids and lipids biosynthesis, promoting tumour growth. Metabolic enzymes upregulated in RCC are labelled yellow. Abbreviations: ACC- Acetyl-coenzyme A carboxylase; FH- Fumarate hydratase; G6PD- Glucose-6-phoshate dehydrogenase; GLS- Glutaminase; GLUT- Glucose transporter; HKII- Hexokinase II; LDHA- Lactate dehydrogenase A; MCT- Monocarboxylate transporter; OAA- Oxaloacetate; PDH- Pyruvate dehydrogenase; PDK- Pyruvate dehydrogenase kinase; PKM2- Pyruvate kinase M2, SDH- Succinate dehydrogenase; SLC1A5- Solute carrier family 1 member 5; TCA- Tricarboxylic acid cycle; TME-Tumour microenvironment; α-KG- Alphaketoglutarate. 7

Figure 6. VHL/HIF axis in ccRCC reprogramming. ccRCC is known for the lack of VHL, promoting HIFs accumulation and translocation to the nucleus where they promote the transcription of cell metabolism, proliferation and angiogenesis genes. Abbreviations: ccRCC- clear cell renal cell carcinoma; VHL- Von Hippel-Lindau; HIF- hypoxia inducible factor. 9

Figure 7. Symbiosis between normal/ normoxic cells and glycolytic/ hypoxic tumour cells. Tumour cells present high glycolytic rates with excessive lactate production, which is transported through MCTs to the TME. Normal cells have the capacity to uptake lactate produced from tumour cells and convert it into pyruvate through LDHB activity. Pyruvate

enters the TCA cycle, functioning as a nutrient source to normal cells, sparing the available glucose in the TME to tumour cells. Abbreviations: GLUT- glucose transporter; MCT- monocarboxylate transporter; TME- tumour microenvironment; LDHB- lactate dehydrogenase B; TCA- tricarboxylic acid cycle; NAD- nicotinamide adenine dinucleotide + hydrogen (H).....11
Figure 8. Lactate functions as an oncometabolite in the TME. Lactate, the end product of glycolysis, is transported to the TME through MCT1 and MCT4. In the TME, contributes to its acidification, which induces invasion and metastasis, immune suppression and resistance to therapy. Lactate can also be used as a source of fuel by cancer cells when glucose is not available. 13
Figure 9. HIF-1α and VHL transcriptional expression, as well as VHL promoter methylation in ccRCC. Transcriptional HIF-1α **(A)** and VHL **(B)** expression in ccRCC compared to normal kidney tissues. **(C)** VHL promoter methylation in ccRCC compared to normal kidney tissues; **p* <0.05; ***p* <0.01 for ccRCC vs normal kidney. 14
Despite the decrease in HIF-1α transcript levels, protein levels were increased in ccRCC and no nuclear expression was detected in normal kidney tissues (Figure 10). Furthermore, all ccRCC cases, except one, lack VHL protein (Figure 10). 14
Figure 10. HIF-1α upregulation and VHL downregulation in ccRCC. Immunohistochemical pictures for HIF-1α **(A)** and VHL **(C)** expression in ccRCC and normal kidney tissues; Graphical representation of HIF-1α **(B)** and VHL **(D)** negative vs positive cases in ccRCC and normal kidney tissues. 15
Figure 11. MCT1 and MCT4 upregulation in ccRCC. (A) Transcriptional MCT1 and MCT4 expression in ccRCC compared to normal kidney tissues; **(B)** Immunohistochemical pictures for MCT1 and MCT4 expression in ccRCC and normal kidney tissues; **(C)** Graphical representation of MCT1 and MCT4 negative vs positive cases in ccRCC and normal kidney tissues; **** *p*<0.0001 for ccRCC vs normal kidney. 16
Figure 12. MCT1 and MCT4 staining intensity in the different tumour stages (I-IV) in ccRCC cases. 17
Figure 13. HIF-2α expression is upregulated in ccRCC and HIF-1α expression increases with disease stage. HIF-2α transcript levels evaluated through RT-qPCR in ccRCC and normal kidney samples **(A)**. HIF-1α **(B)** and HIF-2α **(C)** relative expression in the four grades of ccRCC. Each sample was run in triplicates. *p<0.05; ***p<0.001. 30
Figure 14. Characterization of MCTs and hypoxia-related metabolic markers expression in ccRCC cell lines by Western Blot. Results are representative of 3 independent replicates. Molecular weights: VHL: 20kDa, MCT1: 45kDa, MCT4: 43kDa, HIF-

1α: 120kDa, HIF-2α 115kDa, GLUT1: 45-60kDa, HK2: 102kDa, LDHA: 37kDa, PDK: 47kDa, PKM2: 60kDa and β-actin: 42kDa.....31
Figure 15. MCTs are downregulated in different ccRCC cells after CRISPR/cas9 transfection. CRISPR/Cas9-mediated MCTs knockdown in the obtained clones was confirmed by WB **(A)** and IF for ccRCC cell lines 769-P **(B)**, 786-O **(C)** and Caki-1 **(D)**. Results are representative of three independent replicates. Molecular weights: MCT1: 45kDa, MCT4: 43kDa and β-actin: 42kDa.....33
Figure 16. MCTs knockdown decreases glucose consumption and lactate production in ccRCC. Glucose consumption **(A)** and lactate production **(B)**, over time, in the different MCTs knockdown clones obtained for each ccRCC cell line 769-P, 786-O and Caki-1. Results are the mean of, at least, four independent replicates, each one in triplicates. *p<0.05; **p<0.01 for specific MCTs knockdown clone compared to scramble. 34
Figure 17. MCT1 and MCT4 knockdown show differential metabolic markers expression in ccRCC cells. Characterization of metabolic markers expression by WB **(A)** and IF **(B).** Results are representative of three independent replicates. Molecular weights: GLUT1: 45-60kDa, HKII: 102kDa, LDHA: 37kDa, PKM2: 60kDa and β-actin: 42kDa**.**.....36
Figure 18. HIF-1α and HIF-2α profile for MCT1 and MCT4 knockdown in ccRCC cells. Characterization of hypoxic markers expression by IF**.** Pictures were taken in a fluorescence microscope (Olympus IX51) with a digital camera (Olympus IX81) at 400x magnification. 38
Figure 19. MCTs downregulation promotes decreased cell growth and colony formation in ccRCC. MCTs knockdown effect on tumour growth by Trypan blue dye exclusion assay **(A)** and on the clonogenic capacity **(B)** of ccRCC cells. Results are compared to scramble condition and represents the mean of, at least, five independent experiments. *p<0.05; **p<0.01 for specific MCTs knockdown clone compared to scramble. 39
Figure 20. MCTs knockdown decreases cell proliferation in ccRCC. Graphical representation of MCTs knockdown effect in cell proliferation by BrdU incorporation assay through flow cytometry **(A)**. Representative dot-plots of 769-P, 786-O and Caki-1 cells **(B)** pulsed with 5μg/mL BrdU and then stained with Phase-Flow™ BrdU Cell Proliferation kit. Results are the mean of, at least, three independent experiments. *p<0.05 for specific MCTs knockdown clone compared to scramble. 40
Figure 21. MCTs downregulation promotes a ccRCC cell migration decreasing. Effect of MCTs knockdown in cell migration by wound-healing assay. **(A)** Representative images of cell migration in different time points: 0h, 6h, 12h and 24h and **(B)** graphical representation of MCTs knockdown effect on cell migration capacity. Results are compared

to scramble condition and are the mean of, at least, four independent experiments. *p<0.05 and **p<0.01.....42
Figure 22. MCTs downregulation contributes to decreased invasion capacity in ccRCC cells. Effect of MCTs knockdown in cell invasion by BD Biosciences Matrigel Invasion Chambers assay. Results are compared to scramble condition and are the mean of, at least, four independent experiments. *p<0.05 and **p<0.01.....43
Figure 23. MCTs downregulation effect on EMT-related markers expression for ccRCC cells. The vimentin and β-catenin protein levels were assessed by WB. Results are compared to scramble condition and are the mean of, at least, four independent experiments. Molecular weights: Vimentin: 57kDa, β-catenin: 88kDa and β-actin: 42kDa. 43
Figure 24. MCTs knockdown attenuates the in vivo ccRCC malignant phenotype. Macroscopic view of tumour formation (in ovo and ex ovo) and neo-angiogenesis in 769-P **(A),** 786-O **(B)** and Caki-1 **(C)** scramble and MCTs knockdown experimental conditions. Pictures are representative of three eggs per experimental condition. 44
Figure 25. VHL/HIF- metabolic reprogramming and MCTs expression in ccRCC. VHL absence due to promoter hypermethylation or mutation leads to HIF-1α and HIF-2α accumulation, which promotes glycolysis related genes' transcription. This favours excessive lactate production in ccRCC cells. MCTs knockdown reduces the amount of lactate present in the TME and, consequently, ccRCC cells present lower glycolysic rates which leads to a decrease in tumour growth and proliferation. MCT4 revealed to be a crucial player in sustaining the aggressive phenotype since its knockdown led to reduced tumour migration and invasion. Abbreviations: ccRCC- clear cell renal cell carcinoma; GLUT- glucose transporter; VHL- Von Hippel Lindau; HIF- hypoxia inducible factor; TCA- tricarboxylic acid cycle; MCT- monocarboxylate transporter; TME- tumour microenvironment.….....50

TABLE INDEX

Table 1. MCTs plasma membrane, HIF-1α and VHL expression in ccRCC and normal kidney samples and respective p values. 17
Table 2. Clear cell renal cell carcinoma cell lines used in the work [90]. 19
Table 3. Antibodies used in Western Blot and respective dilutions. 22
Table 4. Antibodies used in the immunofluorescence with fixation and permeabilization methods, respectively. 23
Table 5. Percentage of ccRCC positive cases for the specific VHL mutation “p.F76del c.226_228delTTC”. 29

LIST OF ABBREVIATIONS

4-AP: 4-aminophenazone

7-AAD: 7-Aminoactinomycin D

ACC: acetyl-coenzyme A carboxylase

BAP1: ubiquitin carboxyl-terminal hydrolase

BBB: blood-brain barrier

BrdU: 5-bromo-2'-deoxyuridine

CAM: Chorioallantoic membrane

ccRCC: clear cell renal cell carcinoma

cDNA: DNA complementary

chRCC: chromophobe renal cell carcinoma

DAPI: 4',6- diamidino-2-phenylindole

DNMTs: DNA methyltransferases

EDTA: ethylenediamine tetraacetic acid

EMT: epithelial-mesenchymal transition

FBS: fetal bovine serum

FH: fumarate hydratase

FITC: fluorescein isothiocyanate

FLCN: folliculin

G6PD: glucose-6-phoshate dehydrogenase

GLS: glutaminase

GLUT: glucose transporter

GOD: glucose-oxidase

H_2O_2: hydrogen peroxide

HIF: Hypoxia-inducible factor

HKII: hexokinase II

HRE: hypoxic-response elements

IF: immunofluorescence

IgG: immunoglobulin G

IHC: immunohistochemistry

LDHA: lactate dehydrogenase A

LO: lactate oxidase

MCT: monocarboxylate transporter

MET: mesenchymal-epithelial transition factor

miRNAs: microRNAs

MTT: 3-(4,5-dimethylthiazol-2-yl)-2,5-diphenyltetrazolium bromide

MYC: MYC oncogene

OAA: oxaloacetate

OXPHOS: oxidative phosphorylation

PBS: phosphate-buffer saline

PDH: pyruvate dehydrogenase

PDK: pyruvate dehydrogenase kinase

PE: platting efficiency

PFK: phosphofructokinase

PHD: prolyl hydroxylase proteins

PKM2: pyruvate kinase M2

POD: peroxidase

PPP: pentose phosphate pathway

pRCC: papillary renal cell carcinoma

PTEN: phosphatase and tensin homolog

qPCR: quantitative polymerase chain reaction

qRT-PCR: quantitative reverse transcriptase polymerase chain reaction

RCC: renal cell carcinoma

ROS: reactive oxygen species

RPE: retina pigmented epithelium

SAH: sadenosylhomocysteine

SAM: S-adenosyl-L-methionine

SDH: succinate dehydrogenase

SDHB, SDHC, SDHD: succinate dehydrogenase subunit B, C or D

SDS-PAGE: sodium dodecyl sulfate polyacrylamide gel electrophoresis

SF: survival fraction

SLC16: *Solute Carrier Family 16*

SLC1A5: solute carrier family 1 member 5

TBS-T: tris-buffer saline through 0.1% Tween

TCA: tricarboxylic acid cycle

TET: ten-eleven translocation protein

TM: transmembrane

TME: tumour microenvironment

TRITC: tetramethylrhodamine

TSC: tuberous sclerosis complex

VEGF: vascular endothelial growth factor

VHL: Von Hippel-Lindau

WB: western blot

WHO: World Health Organization

α-KG: alphaketoglutarate

INTRODUCTION

1.1. Kidney cancer

1.1.1. Epidemiology

Kidney cancer, also known as renal cell carcinoma (RCC), is the most recurrent solid lesion within the kidney and represents around 3% of all cancers worldwide, having been diagnosed approximately 431000 new cases and 179000 deaths in 2020 (via Globocan). The incidence rates are generally higher in developed countries and have doubled over the past 50 years [1], while the mortality rates have been decreasing since the 1990s. Men are more affected than women and the average age of diagnosis in the US is 64 years-old. However, the possibility of a hereditary kidney cancer syndrome is considered when RCC is diagnosed 20 years earlier [2].

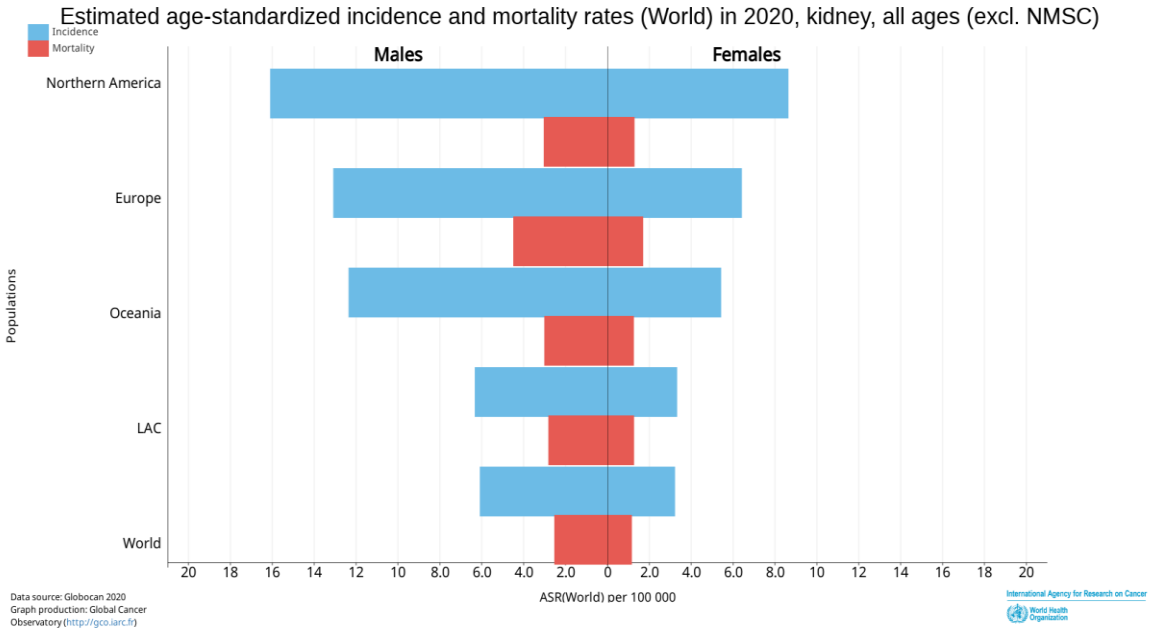

Figure 1. Worldwide RCC incidence and mortality distributions. 2020 global incidence (blue) and mortality (red) rates for both sexes estimated age-standardized. Via Globocan.

1.1.2. Diagnosis and treatment

Most patients with RCC only present symptomatic disease in advanced stages. In fact, most of the cases are detected incidentally by abdominal ultrasound scanning or computed tomography imaging during routine evaluation. However, some patients are presented with symptoms such as persistent cough, bone pain or palpable abdominal masses [3]. Besides, RCC are typically linked with paraneoplastic syndromes such as hypertension, anemia and cachexia [4]. 20% of the patients already present metastases at the time of diagnosis, however

most RCC cases are diagnosed at early stages. In so, the 5-year survival rates are higher than 85% but decrease to less than 20% when it comes to metastatic disease [5].

Localized RCC can be treated with partial or radical nephrectomy whereas metastatic cases are managed with conventional chemotherapy [6]. Nevertheless, in the past decades the increased understanding in genomic and molecular behavior of the disease has allowed the development of alternative target therapies. Antiangiogenic agents, like tyrosine kinase inhibitors targeting the vascular endothelial growth factor (VEGF) signalling pathway, are currently available due to the strong vascularization present in RCC. Furthermore, mTOR inhibitors as well as immune checkpoint inhibitors have been also used with improvements in response rates [7]. However, patient response to treatment is variable and RCC is still associated with high recurrence rates [2]. Importantly further investigation underlying tumour heterogeneity and its molecular biology is needed in order to identify new tumour-associated markers that allow the development of new therapeutic strategies for RCC patients' clinical management.

1.1.3. Risk factors

RCC incidence increases with age and two-thirds of the diagnoses are made in men. The established modifiable risk factors include excess body weight, smoking, diet, alcohol consumption and hypertension [2]. Although most kidney tumours are sporadic, genetic factors also play an important role in its development and progression, as demonstrated by the two-fold increased risk of RCC in individuals with a familial history of renal cancer [2, 8]. At least 11 genes (*VHL, PTEN, MET, BAP1, FH, TSC1, TSC2, SDHB, SDHC, SDHD and FLCN*) have been discovered to uncover mutations which are associated with familial RCC. The most notable example is the Von Hippel-Lindau (*VHL)*, which encodes pVHL, that is involved in several different metabolic pathways [9]. Inactivation of VHL protein leads to constitutive activation of the oncogenic hypoxia-inducible factors (HIFs) expression involved in clear cell renal cell carcinoma (ccRCC) development [10].

1.2. Renal cell carcinoma classification

RCC is not a single disease but a heterogeneous cancer, with different histology, genetic and epigenetic alterations [2, 11]. Renal cell tumours classification has been recently revised by the World Health Organization (WHO), which had in consideration the identification of novel features relying pathology, epidemiology and genetics [12]. Clear cell renal cell carcinoma, papillary renal cell carcinoma (pRCC) and chromophobe renal cell carcinoma (chRCC) are the most common forms of the disease, with the first two holding together approximately 90% of

all cases. Collecting duct, translocation and medullary carcinomas are rare histological subtypes worth less than 1% of RCC [13]. These RCC types have different clinical courses and responses to therapy and different studies have shown that ccRCC has the worst outcome of all [13, 14].

1.2.1. Clear Cell Renal Cell Carcinoma

ccRCC is the most frequent subtype of renal cancer with necrotic areas usually associated with increased tumour aggressiveness. These tumours most commonly metastasize to the lung and are known for its late metastasis, that can occur even 10 years after the diagnosis [15]. In fact, RCC, and ccRCC in particular, is the most lethal urological tumour, with a 5-year survival rate below 10% for metastatic disease, mostly due to the limited efficacy of available therapies. ccRCC are known for the lack of the *VHL* suppressor gene located in chromosome 3p (3p25-26) [16]. This gene encodes VHL protein that is involved in several different metabolic pathways such as the glutamine metabolism, the tricarboxylic acid (TCA) cycle and tumour energetics [9]. In 90% of sporadic ccRCCs, one copy of VHL is either silenced or mutated and the other copy is generally lost through 3p deletions [13]. Indeed, *VHL* biallelic inactivation caused by genetic mutations or by promoter hypermethylation is a driving event in ccRCC initiation and progression [17]. Being so, ccRCC can be considered a metabolic disease and, in some cases, epigenetic modifications can lead to malignant cellular transformation.

1.3. Epigenetic

The term epigenetics was introduced by Conrad Waddington in the early 1940s. He defined it as ‘‘the branch of biology which studies the causal interactions between genes and their products which bring the phenotype into being”. However, this definition has evolved over time and, nowadays, we can say that epigenetic is “the study of heritable changes in gene expression that occur independent of changes in the primary DNA sequence” [18]. There are different types of epigenetics mechanisms, which regulate several DNA/RNA mediated processes, including transcription, DNA repair and DNA replication, through modulation of the chromatin structure. These mechanisms can be divided into different categories: alteration in histone structure through post-translational modifications, incorporation of histone variants, non-coding RNAs including microRNAs (miRNAs) and DNA methylation (Figure 2), the one we are focusing in this work. These modifications work together to regulate the functioning of the genome, regulating chromatin’s accessibility and compactness [19, 20] and are extremely important for the normal development and maintenance of tissue-specific gene expression patterns. In fact, its disruption can lead to altered gene function and malignant cellular

transformation [19]. Thus, epigenetic modifications represent promising therapeutics targets and its study underlying tumourigenesis has been a challenge for researchers.

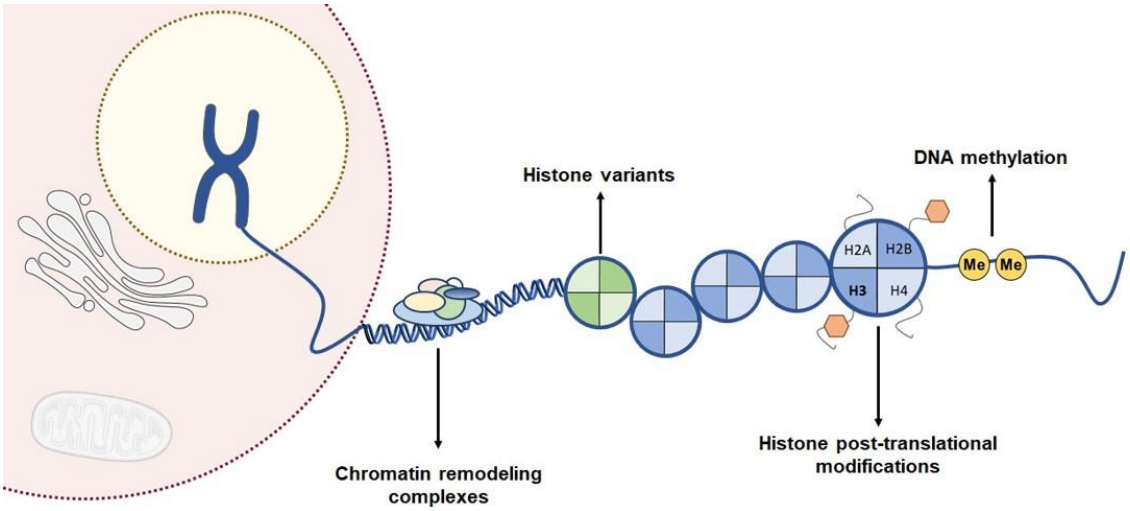

Figure 2. Epigenetic mechanisms involved in gene expression regulation. Chromatin remodeling complexes, histone variants, histone post-translational modifications and DNA methylation regulate gene transcription through chromatin structure modulation. Adapted from [21].

1.3.1. DNA methylation

DNA methylation is one of the major epigenetic modifications studied in cancer and so far in ccRCC development. DNA methylation occurs by the covalent modification of cytosine residues in CpG dinucleotides. CpG dinucleotides are not evenly distributed across the human genome but are instead concentrated in regions with high frequency of CpG sites called CpG islands [19, 22]. The genomic methylation process consists in the addition of a methyl group to cytosine and it is mediated by DNA methyltransferases (DNMTs), using a methyl donor S-adenosyl-L-methionine (SAM) (Figure 3) [22]. This process is dynamic and can be reversed by the ten-eleven translocation protein (TET) which mediates the DNA demethylation by adding a hydroxyl group to 5'methyl-cytosine (Figure 3).

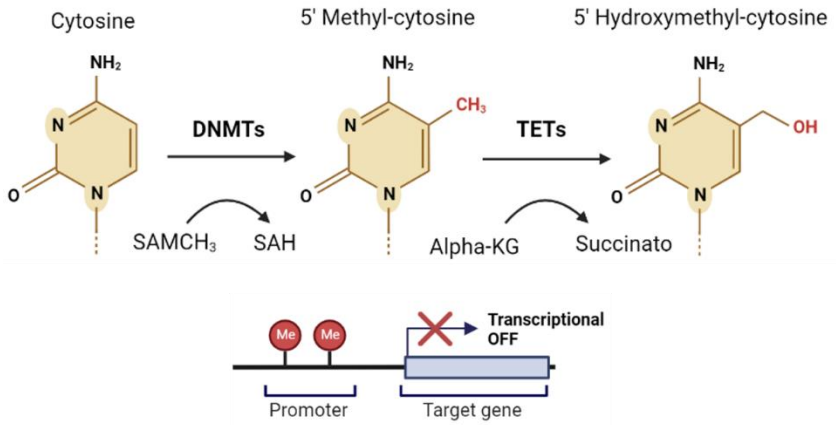

Figure 3. DNA methylation regulation. DNMTs catalyse cytosine methylation using SAM as a methyl donor and reducing it to SAH. TETs revert DNA methylation by converting 5'Methyl-Cytosine into 5'Hydroxymethyl-Cytosine through a hydroxylation α-ketoglutarate dependent reaction. Gene promoter hypermethylation inhibits transcription. Abbreviations: DNMT- DNA methyltransferase; SAH- S-adenosylhomocysteine; SAM- S-adenosyl-L-methionine; TET- Ten-eleven translocation.

In normal cells, about 60% of the gene promoters are unmethylated and associated with CpG islands [22]. However, some CpG island promoters become methylated during development resulting in transcriptional silencing. On the other hand, DNA methylation can lead to transcriptional activation when it occurs at CG-poor regions within gene bodies [23]. Several studies have shown that deregulation of DNA methylation process is involved in cancer development and growth [23]. In general, cancer cells are characterized by a global loss of DNA methylation when compared to the non-tumour cells. However, we can observe the acquisition of specific hypermethylation patterns at the CpG islands of some gene promoters. Therefore, we can identify two patterns of methylation in cancer: global hypomethylation of DNA and specific hypermethylation of some CpG islands [23].

This specific epigenetic deregulation is frequent in RCC [24]. As previously mentioned, epigenetic alterations, namely CpG islands hypermethylation, in the *VHL* promoter are an important event in ccRCC initiation [9]. This mechanism has been studied in ccRCC over the years and *VHL* promoter hypermethylation has been reported in 11% of the cases [25].

1.4. Tumour cell metabolism

Deregulation of cell metabolism constitutes a well-established cancer hallmark (Figure 4) that contributes to tumour initiation and progression, since cancer cells rewire their metabolism to promote growth, proliferation, and survival [26].

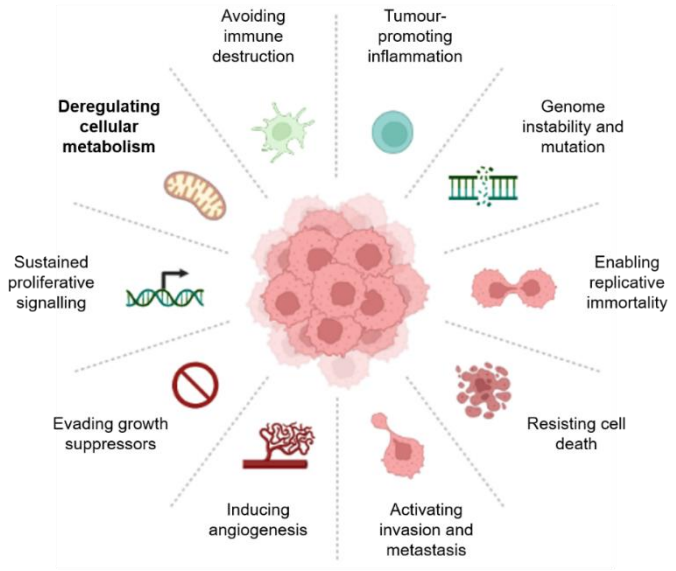

Figure 4. Hallmarks of cancer. The cancer hallmarks comprise biological mechanisms adaptations that cancer cells rewire to favoring tumour growth and aggressiveness.

In normal cells, glycolysis is reduced in the presence of oxygen and energy production comes from oxidative phosphorylation (OXPHOS) [21]. However, tumour cells alter their metabolism increasing glucose uptake and its fermentation to lactate, even in the presence of oxygen. Thus, these cells have a low oxidative profile because they tend to favor aerobic glycolysis rather than the OXPHOS pathway, a phenomenon known as “Warburg effect” [27]. As a result, there is an upregulation of genes involved in glycolysis and cancer cells convert the great majority of the incoming glucose into lactate rather than into pyruvate [28].

Within a bioenergetics theory, this glycolytic phenotype is less efficient than the OXPHOS since it produces less ATP molecules. However, the Warburg phenotype confers numerous adaptive advantages to cancer cells: these cells show an increased survival capacity in fluctuating oxygen levels; they use the excess of carbon for anabolic reactions, allowing the *de novo* nucleotides, lipids and amino acids generation [26, 27]. The Warburg effect also allows cells to maintain the appropriate balance of reactive oxygen species (ROS), protecting them from oxidative stress. Furthermore, it increases lactate production and, consequently, acidifies the tumour microenvironment (TME) which leads to immunosuppression and supports cancer cells’ aggressiveness through increased migration, invasion and metastasis [26].

1.4.1. Metabolic alterations in RCC

Several RCC mutations play an important role in metabolic reprogramming of these tumours, namely FH and SDH genes, which promote accumulation of fumarate or succinate, respectively, leading to prolyl hydroxylase (PHD) inhibition and HIF-1α stabilization [29]. In

addition, loss of VHL function is also found in the majority of RCC cases. VHL inactivation leads to constitutive HIFs activation promoting a pseudo-hypoxia status. Hence, these tumours overexpress glycolytic enzymes that allow to maintain a highly glycolytic metabolism. Besides glycolysis, other metabolic enzymes related to glutaminolysis, fatty acids metabolism and pentose phosphate pathway (PPP) are also deregulated in RCC (Figure 5) [30, 31]. The PPP provides ribose needed for nucleotide biosynthesis and are crucial in defence against oxidative stress and apoptosis [32]. Additionally, enzymes of fatty acids synthesis pathway were found increased in RCC and associated with tumour aggressiveness and poor prognosis [33]. Furthermore, MYC oncogene (MYC) overexpression induces glutamine transporter (SLC1A5) and glutaminase (GLS) upregulation [34], promoting alterations in RCC' glutamine metabolism (Figure 5).

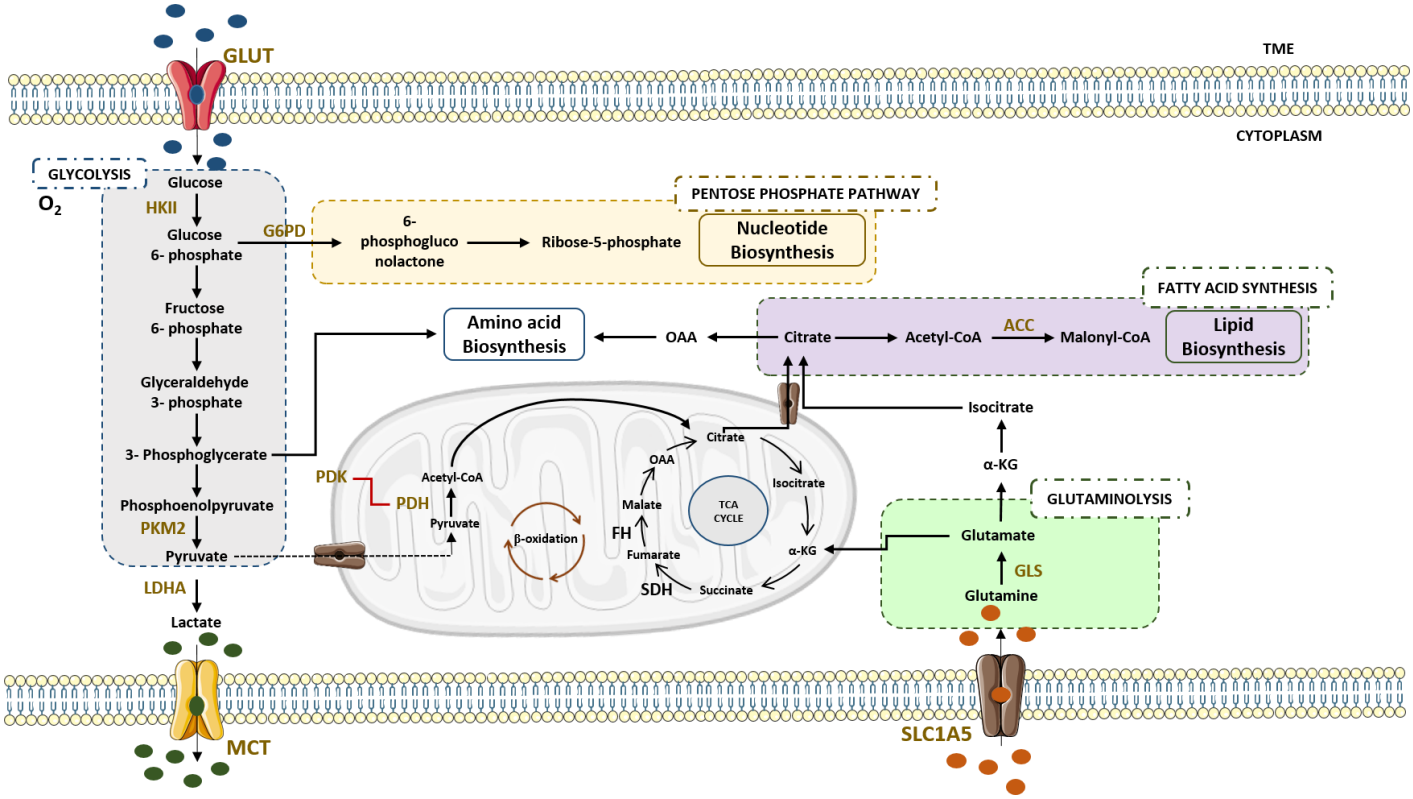

Figure 5. Metabolic reprogramming in RCC. Renal cell carcinomas are characterized by a high glycolytic phenotype with increased glucose uptake and lactate production. Pentose phosphate pathway, fatty acid synthesis and glutaminolysis are increased to sustain nucleotides, amino acids and lipids biosynthesis, promoting tumour growth. Metabolic enzymes upregulated in RCC are labelled yellow. Abbreviations: ACC- Acetyl-coenzyme A carboxylase; FH- Fumarate hydratase; G6PD- Glucose-6-phoshate dehydrogenase; GLS- Glutaminase; GLUT- Glucose transporter; HKII- Hexokinase II; LDHA- Lactate dehydrogenase A; MCT- Monocarboxylate transporter; OAA- Oxaloacetate; PDH- Pyruvate dehydrogenase; PDK- Pyruvate dehydrogenase kinase; PKM2- Pyruvate kinase M2, SDH- Succinate dehydrogenase; SLC1A5- Solute carrier family 1 member 5; TCA- Tricarboxylic acid cycle; TME-Tumour microenvironment; α-KG- Alphaketoglutarate.

1.4.2. Metabolic reprogramming in ccRCC

VHL role in the regulation of HIF-1α was first demonstrated by Maxwell et al [35]. More recently, some studies have shown that both HIF-1α and HIF-2α are involved in ccRCC initiation and the expression of both is regulated by VHL [36]. *VHL* encodes VHL protein which is part of a ligase complex that binds to HIFs. This transcription factor is a heterodimer composed of an oxygen dependent α subunit and a constitutively expressed non-oxygen dependent β subunit [37]. Under normal conditions, PHD proteins catalyze proline residues hydroxylation on HIFs, which allow VHL binding to these proteins leading to its ubiquitination and proteasomal degradation. However, under hypoxia conditions PHD are inactive and, consequently, HIFs are not hydroxylated [38].

Being so, VHL does not bind to HIFs, which allows them to interact with HIF-1β present in the nucleus, forming a HIF-1α/β complex, which posteriorly binds to target genes on their hypoxic-response elements (HRE). This binding promotes the transcription of genes involved in the regulation of cell metabolism, cell proliferation and angiogenesis (Figure 6) [9]. Thus, constitutive HIF-1α activation leads to glycolysis related genes upregulation, such as glucose transporters (GLUT1 and GLUT3), hexokinases (HKII and HKIII), phosphofructokinase (PFK), pyruvate kinase M2 (PKM2) and pyruvate dehydrogenase kinase (PDK), favoring the glycolytic metabolism [39]. Furthermore, lactate dehydrogenase A (LDHA) is also upregulated by HIF-1α contributing to an increased lactate production. To prevent intracellular acidification, HIF-1α induces the expression of MCTs, particularly MCT4 [40-42] and lactate is transported to the TME contributing to its acidification, leading to increased proliferation and aggressiveness, resulting in poor prognosis and resistance. On the other hand, there is some evidence showing that lactate can stimulate HIFs accumulation, independently from hypoxia, resulting from a positive feedback [36]. Thus, unveiling the role of VHL/HIF- dependent metabolic profile interplay in ccRCC carcinogenesis and metastasis development may allow for identification of new therapeutic targets.

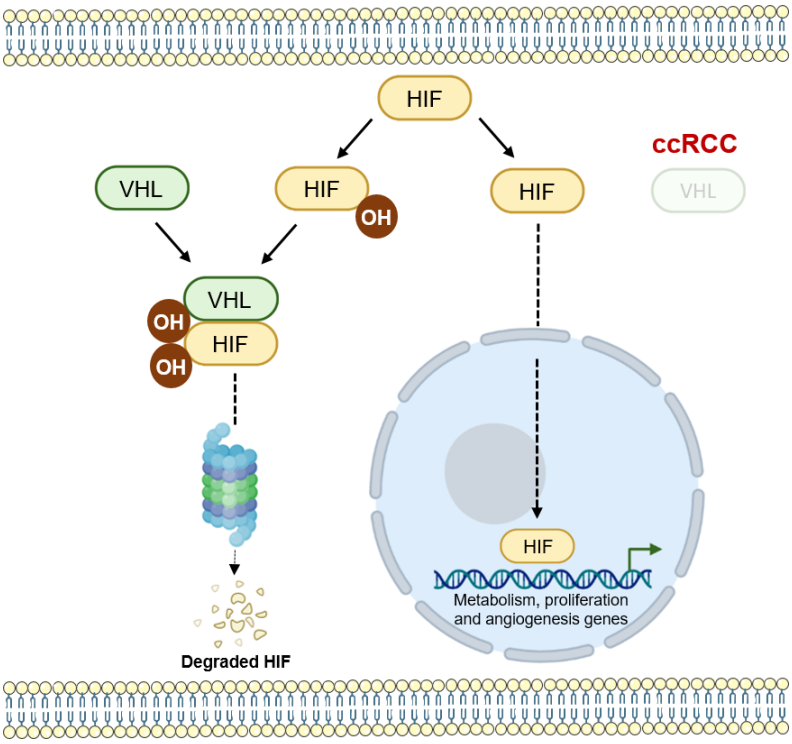

Figure 6. VHL/HIF axis in ccRCC reprogramming. ccRCC is known for the lack of VHL, promoting HIFs accumulation and translocation to the nucleus where they promote the transcription of cell metabolism, proliferation and angiogenesis genes. Abbreviations: ccRCC- clear cell renal cell carcinoma; VHL- Von Hippel-Lindau; HIF- hypoxia inducible factor.

1.5. Monocarboxylate transporters family

Monocarboxylates play an important role in the metabolism of all cells, with lactate having a key function in it. Its transport is mediated by MCTs, a family of monocarboxylate transporters that is encoded by the *Solute Carrier Family 16 (SLC16)* gene comprising 14 isoforms [43]. Within these, only MCT1-MCT4 have been demonstrated experimentally to facilitate the proton-linked transport of metabolic monocarboxylic acids, like lactate [44]. Lactic acid is the major metabolic product from aerobic glycolysis in cancer. Since the pK value of lactic acid is 3.86, this charged species cannot cross the plasma membrane by free diffusion, but requires a specific transport mechanism, namely through MCTs [45]. Thus, MCTs catalyse the facilitated diffusion of lactate with a proton by a symport mechanism. The transport is performed by an ordered mechanism in which H^+ binding precedes monocarboxylate binding to the protonated transporter [46]. Structurally, MCTs have 12 transmembrane (TMs) domains with a large cytosolic loop between TMs 6 and 7, an intracellular hydrophilic C- and N-termini [47]. The former are the most conserved and the hydrophilic regions show little conservation, indicating that they are unlikely to be directly involved in the transport, being critical in other functional aspects such as substrate affinity or in activity regulation [48].

MCTs have a central role in mammalian cell metabolism and in the communication between cells, therefore having different properties, tissue distribution and being differently regulated [47]. Even though lactate is the major monocarboxylate transported across the plasma membrane, the proton-coupled isoforms MCT1-4 also transport other metabolically important monocarboxylates, such as pyruvate and ketone bodies, hormones and amino acids [49]. Some studies regarding MCT1 and MCT4 upregulation in tumour cells have been carried out, showing a positive association between this upregulation and poor prognosis in multiple malignant tumours [50-52]. Nevertheless, MCT2 and MCT3, have been less described in cancer when compared to the other proton-coupled isoforms [44]. Being so, this work is only focused on the current roles of MCT1 and MCT4 in tumour cells and its potential as targets in cancer, particularly in ccRCC.

1.5.1. MCT1 and MCT4 metabolic roles in tumour cells

MCT1 and MCT4 are the most widely MCT isoforms expressed in tumour cells, having a particularly important role in the maintenance of the metabolic phenotype of these cells. Besides facilitating the efflux of lactate, they also contribute to the intracellular pH preservation, by co-transporting a proton. However, MCT1 and MCT4 differ in aspects such as tissue distribution and biochemical properties [44, 46]. MCT1, encoded by *SLC16A1* gene, is the most well studied member of the MCT family, being the only one expressed in human erythrocytes [47, 48]. MCT1 has an ubiquitous distribution in human tissues, with higher expression in heart and muscle, being also present in blood-brain barrier (BBB), apical membrane of retina pigmented epithelium (RPE), kidney, stomach, liver, gut epithelium and T-lymphocytes [48]. MCT4, encoded by *SLC16A3,* is particularly important in highly glycolytic tissues that need to export lactic acid. In fact, MCT4 is expressed in neonatal heart which is more glycolytic than adult heart [53]. Besides, MCT4 is abundant in skeletal muscle fibres, white blood cells, astrocytes and chondrocytes [47, 54]. MCTs deregulation has been reported in different human cancers, such as gliomas [55], bladder [56], stomach [57, 58], head and neck [59, 60], prostate [61], breast [62], cervix [63], ovary [64], colorectal [65] and melanoma [66, 67]. Although not much is known about MCTs involvement in RCC, some studies have been carried out over the years. Indeed, GLUT1, MCT1 and MCT4 overexpression has been shown to support the glycolytic metabolism in pRCC with MCT1 overexpression contributing to pRCC aggressiveness [68]. Recently, GLUT1 and MCT1 were also identified as poor prognosis factors in ccRCC [69-71]. However, an important MCT4 role in ccRCC aggressiveness has also been described [70-73].

MCT1 and MCT4 display, respectively, high and low affinity for lactate [44] and can operate bidirectionally, depending on the substrate concentration [43]. More recently, it was described that MCT1 is associated with both lactate efflux and influx whilst MCT4 is more likely to be involved only in lactate export from tumour cells [54]. Furthermore, MCT4 has low affinity for pyruvate, which prevents its efflux from the cell, allowing lactate generation through LDHA activity and, consequently, the maintenance of the glycolytic phenotype [53]. As previously described, the TME is composed not only by tumour cells but also by normal cells. And, since the former have high glycolytic rates, normal cells have the capacity to uptake lactate-derived from cancer cells and convert it into pyruvate through LDHB, a LDH subunit [74] (Figure 7). Pyruvate is then used as a nutrient source for oxidative phosphorylation, thus sparing the available glucose in the TME for tumour cells. This lactate shuttle has also been reported between hypoxic and normoxic sites: the hypoxic tumour cells dependent on glucose produce high levels of lactate that is exported out of the cell through MCT4 and imported to oxidative tumour cells via MCT1 [44, 74]. This allows cancer cells to maintain their energy production rates, even in nutrient deprived conditions, highlighting the fact that MCT1/4 may be crucial for tumour growth, proliferation, and invasion.

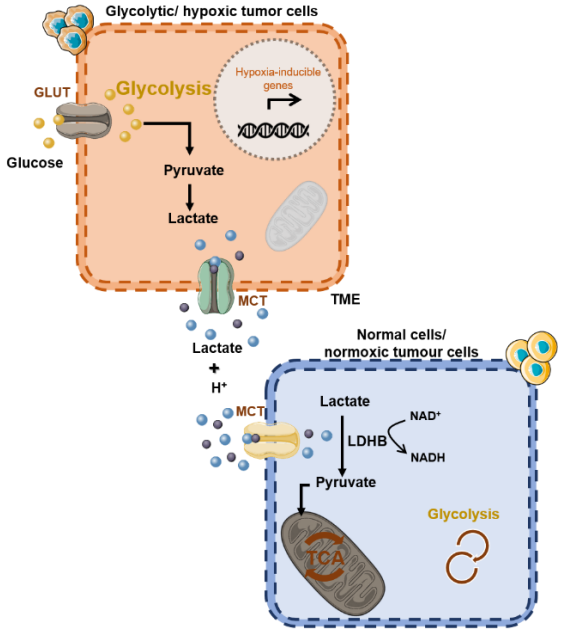

Figure 7. Symbiosis between normal/ normoxic cells and glycolytic/ hypoxic tumour cells. Tumour cells present high glycolytic rates with excessive lactate production, which is transported through MCTs to the TME. Normal cells have the capacity to uptake lactate produced from tumour cells and convert it into pyruvate through LDHB activity. Pyruvate enters the TCA cycle, functioning as a nutrient source to normal cells, sparing the available glucose in the TME to tumour cells. Abbreviations: GLUT- glucose transporter; MCT- monocarboxylate transporter; TME- tumour microenvironment; LDHB- lactate dehydrogenase B; TCA- tricarboxylic acid cycle; NAD- nicotinamide adenine dinucleotide + hydrogen (H).

1.5.2. Lactate in tumour microenvironment

A high glycolytic phenotype is a common feature of solid tumours, like ccRCC, which culminates in excessive lactate production. Owing to lactate efflux through MCTs to the TME, tumour cells maintain the high glycolysis rates that are crucial for cell growth and proliferation [45, 47]. In TME lactate acts as an oncometabolite by lowering the pH to 6.0-6.5 [75, 76], contributing to extracellular acidosis, which favours processes such as metastasis, angiogenesis, immunosuppression and consequently tumour growth and therapy resistance (Figure 8). Furthermore, lactate has been shown to promote the epithelial-mesenchymal transition (EMT) [77] which occurs when neoplastic cells of epithelial origin transiently switch to a mesenchymal-like phenotype in order to gain enhanced migratory capacity, invasiveness, stemness, resistance to apoptosis and greatly increased production of ECM components, such as vimentin and β-catenin [78].

On a different note, lactate can also function as a signalling molecule in a glycolytic and oxidative tumour cell symbiosis, contributing to HIF-1α stabilization [46, 79]. Being so, HIF-1α is active in oxidative tumour cells, independently of the hypoxia conditions, increasing the transcription and release of vascular endothelial growth factor (VEGF), inducing endothelial cells migration and tumour angiogenesis [74]. Indeed, HIF-1α stabilization by lactate promotes an increased VEGF and kinase insert domain receptor VEGFR2 expression by tumour cells and endothelial cells, respectively [79]. Moreover, lactate uptake from TME contributes to interleukin 8 (IL-8) production by endothelial cells driven tumour angiogenesis [80]. As previously described, the lactate present in the TME can lead to immune evasion. In fact, lactate secretion from tumour cells seems to have an important role in macrophage polarization through a M2-phenotype, that has immunosuppressive properties [81]. Furthermore, high lactate levels in the TME block lactate export from T cells that rely on their highly glycolytic phenotype to support their effector functions and proliferative phase [82]. Hence, MCTs have an important role in tumour aggressiveness and are emerging as promising therapeutic targets for cancer treatment.

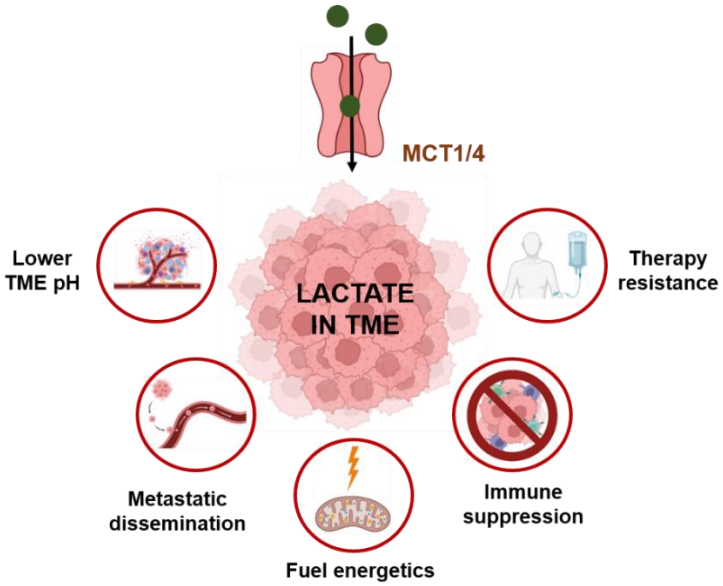

Figure 8. Lactate functions as an oncometabolite in the TME. Lactate, the end product of glycolysis, is transported to the TME through MCT1 and MCT4. In the TME, contributes to its acidification, which induces invasion and metastasis, immune suppression, and resistance to therapy. Lactate can also be used as a source of fuel by cancer cells when glucose is not available. Created with Biorender.com.

1.6. MCTs as therapeutic targets in cancer

Taking all this into account, in the absence of VHL, cells display a hypoxic behavior, even if they possess normal O_2 levels, and present a glycolytic phenotype. Consequently, HIFs accumulate in the nucleus and this deregulation creates a perfect environment for tumour proliferation, migration, and invasion, with MCTs having an important role by transporting lactate into the TME, leading to an increased tumour aggressiveness [43]. In fact, considering MCTs' role in tumour metabolism and homeostasis, its inhibition will end the favourable symbiosis between hypoxic and oxidative tumour cells, slowing down tumour growth [83]. Evidence show that MCT1 inhibition directly decreases intracellular pH leading to cell death [84] and MCT4 silencing decreases cell migration and invasion [85]. Recently, it has been found that silencing MCT1 and MCT4 can restore T cell function and boost immune response in melanoma patients [86]. Additionally, silencing of MCT4 results in decreased cancer cell migration, by mechanisms that involve its interaction with β-integrin [87]. Furthermore, combined silencing of MCT1 and MCT4 inhibited cancer cell invasion [88] and tumour growth by reducing the glycolytic flux [80] in gliomas. Thus, proton-coupled MCTs, mainly MCT1 and MCT4, are emerging as promising therapeutic targets for cancer treatment. However, it has not been described how they are deregulated in ccRCC and how its deregulation is involved in ccRCC aggressiveness.

PRELIMINARY RESULTS

RCC are pseudo-hypoxic tumours with a characteristic glycolytic phenotype, being VHL loss a common feature of these tumours, particularly in ccRCC. Thus, concerning the main group' goals, a characterization of VHL, HIF-1α and MCTs, namely MCT1 and MCT4 isoforms, in a retrospective ccRCC series from Portuguese Oncology Institute of Porto (IPO-Porto) was previously performed by our research team.

VHL and HIF-1α characterization in ccRCC samples

A downregulation in HIF-1α and VHL transcript levels, as well as an increase in VHL promoter methylation levels in ccRCC when compared to normal kidney samples was observed (Figure 9).

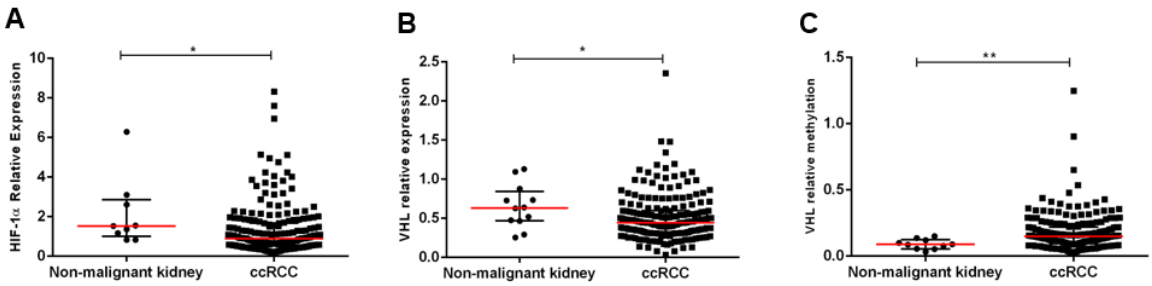

Figure 9. HIF-1α and VHL transcriptional expression, as well as VHL promoter methylation in ccRCC. Transcriptional HIF-1α **(A)** and VHL **(B)** expression in ccRCC compared to normal kidney tissues. **(C)** VHL promoter methylation in ccRCC compared to normal kidney tissues; *p <0.05; **p <0.01 for ccRCC vs normal kidney.

Despite the reduced HIF-1α transcript levels, protein levels were higher in ccRCC and no nuclear expression was detected in normal kidney tissues (Figure 10). Furthermore, all ccRCC cases, except one, lacked VHL protein (Figure 10).

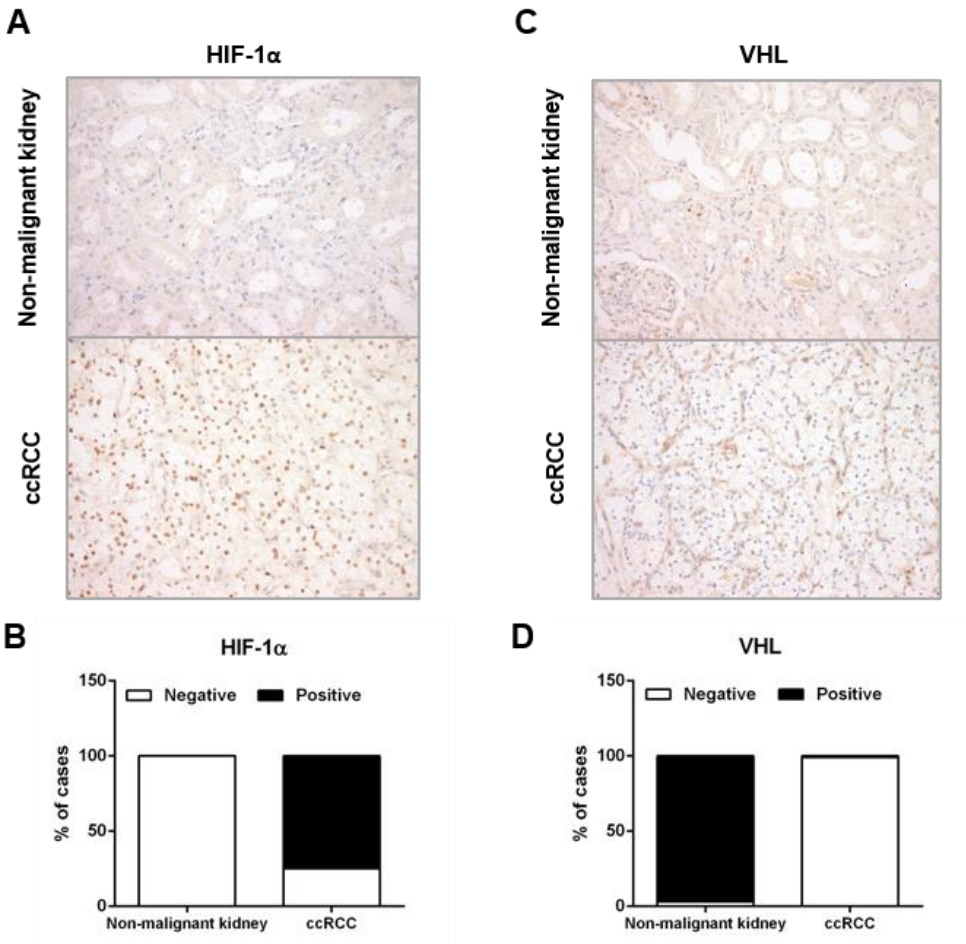

Figure 10. HIF-1α upregulation and VHL downregulation in ccRCC. Immunohistochemical pictures for HIF-1α **(A)** and VHL **(C)** expression in ccRCC and normal kidney tissues; Graphical representation of HIF-1α **(B)** and VHL **(D)** negative vs positive cases in ccRCC and normal kidney tissues.

MCT1 and MCT4 characterization in ccRCC samples

Higher MCT1 and MCT4 expression was found in ccRCC when compared to normal kidney tissues, both at transcript and protein levels (Figure 11). Despite normal kidney expressing MCT1, the staining was in the cytoplasm. However, MCTs function as lactate transporter is dependent on its expression at the plasma membrane, having only been considered the plasma membrane staining for the final immuno-expression score. Being so, ccRCC expressed higher percentage of positive cases for MCT1 and MCT4 plasma membrane expression than the normal kidney tissues, with this increase being more notable in MCT4 (Figure 11B and C and Table 1).

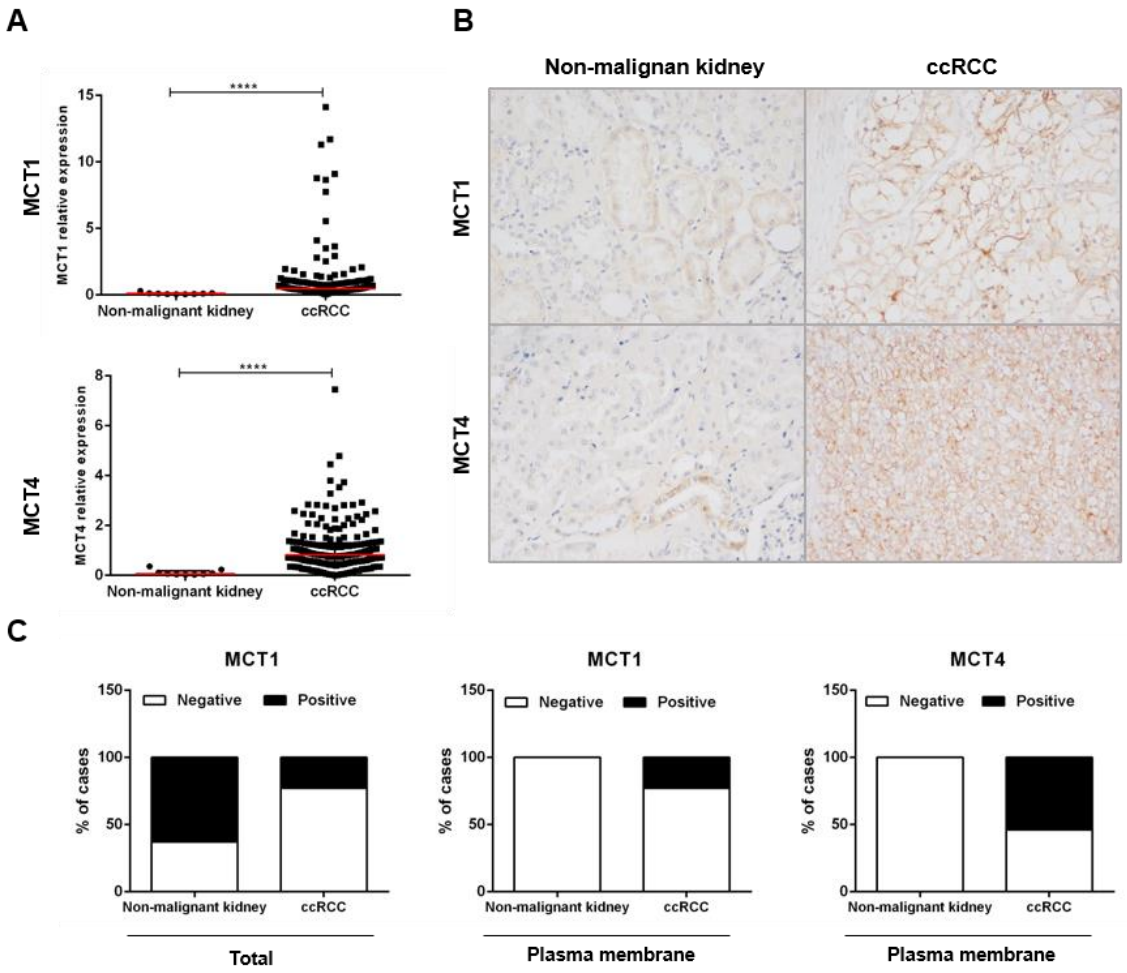

Figure 11. MCT1 and MCT4 upregulation in ccRCC. (A) Transcriptional MCT1 and MCT4 expression in ccRCC compared to normal kidney tissues; **(B)** Immunohistochemical pictures for MCT1 and MCT4 expression in ccRCC and normal kidney tissues; **(C)** Graphical representation of MCT1 and MCT4 negative vs positive cases in ccRCC and normal kidney tissues; **** p<0.0001 for ccRCC *vs* normal kidney.

Table 1. MCTs plasma membrane, HIF-1α and VHL expression in ccRCC and normal kidney samples and respective p values.

		Normal Kidney	ccRCC
MCT1	n	30	200
	Negative (%)	30 (100)	155 (77.5)
	Positive (%)	0 (0)	45 (22.5)
	***p* value**	0.0001	
MCT4	n	30	200
	Negative (%)	30 (100)	93 (46.5)
	Positive (%)	0 (0)	107 (53.5)
	p value	<0.0001	
HIF-1α	n	30	200
	Negative (%)	30 (100)	51 (25.5)
	Positive (%)	0 (0)	149 (74.5)
	p value	<0.0001	
VHL	n	30	200
	Negative (%)	1 (3.3)	199 (99.5)
	Positive (%)	29 (96.7)	1 (0.5)
	p value	<0.0001	

Furthermore, MCTs expression was different within tumour stage. Despite not statistically different, MCT4 staining intensity was higher in more advanced stages of the disease, whereas MCT1 staining intensity did not change over the tumour stage, presenting few cases with staining intensity of 3.

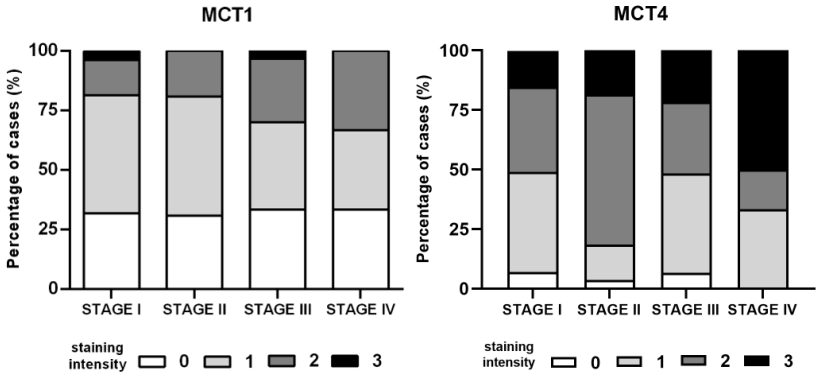

Figure 12. MCT1 and MCT4 staining intensity in the different tumour stages (I-IV) in ccRCC cases.

AIMS

VHL loss is a common characteristic of ccRCC tumours, which leads to constitutive HIF activation promoting a pseudo-hypoxia status. A hypoxic-related metabolic reprogramming, such as the glycolytic enzyme's upregulation, has been described in ccRCC [39]. Although MCTs deregulation has been reported in different tumours, few studies have been carried out in ccRCC [89]. Importantly, as pre-liminary results, our group observed a MCT1 and MCT4 upregulation in ccRCC when compared to normal kidney tissues. Furthermore, almost all ccRCC cases lacked VHL protein expression with concomitant VHL promoter methylation increasing when compared to normal kidney samples. However, the association between VHL/HIF status and metabolic profile in ccRCC has never been addressed, particularly concerning its impact in aggressiveness and progression features. Importantly, unveiling the role of VHL/HIF- dependent metabolic profile interplay in ccRCC carcinogenesis and metastasis development may allow the identification of new therapeutic targets.

Hence, our main goal is to understand the interplay between VHL mutation and/or hypermethylation status and the glycolytic phenotype, specifically MCTs deregulation in the ccRCC aggressiveness. Accordingly, the specific aims for the project are:

1. Evaluate the effect of the VHL/HIF status in the ccRCC metabolic profile

- Characterize the *VHL* mutations status, in a series of ccRCC patients' tissues.
- Analyze the expression of related hypoxia markers in the same set of samples.

2. Explore the interplay between VHL/HIF status and MCTs regulation in ccRCC tumourigenesis

- Characterize the metabolic profile and MCTs expression in ccRCC cell lines with different VHL status.
- Evaluate the *in vitro* impact of specific MCTs inhibition on tumour aggressiveness.
- Assess the role of MCTs *in vivo* tumour formation and progression.

MATERIALS AND METHODS

4.1. Cell lines culture

The ccRCC cell lines (Caki-1, 769-P, and 786-O) obtained from American Type Culture Collection (ATCC) were used (Table 2) in *in vitro* and *in vivo* performed studies. In order to normalize the available glucose quantity, all cell lines were maintained in RPMI-1640 Medium (PAN-Biotech, UK) supplemented with 10% fetal bovine serum (FBS, MERK, Germany) and 1% penicillin/streptomycin (PAN-Biotech, UK) at 37ºC and 5% CO_2 in a humidifying chamber.

Table 2. Clear cell renal cell carcinoma cell lines used in the work [90].

Clear cell renal cell carcinoma cell lines		
	Characteristics	***VHL status***
Caki-1	Metastatic clear cell renal cell carcinoma	Wild-type
769-P	Primary clear cell renal cell carcinoma	Point mutation and methylation
786-O	Primary clear cell renal cell carcinoma	Deletion

4.2. Tissue samples

For the proposed work, a series of 200 ccRCC tissue samples, available at Portuguese Oncology Institute of Porto (IPO Porto) Biobank, collected from patients submitted to radical or partial nephrectomy at the IPO Porto, were included. Additionally, a set of 30 morphologically normal kidney (cortical) samples from nephrectomy specimens obtained from patients with low stage upper urinary tract urothelial carcinoma were used as controls. Informed consent was obtained, and the anonymity of the donor will be safeguarded, in accordance with the ethical principles of the declaration of Helsinki. Patients' data will be kept in strict confidentiality and may be removed from the database at any time, according to patient decision. This study was approved by the Institutional Review Board (Comissão de Ética para a Saúde) of Portuguese Oncology Institute of Porto (CES IPO: 372/2017).

4.3. DNA extraction and quantitative polymerase chain reaction (qPCR)

DNA extraction from ccRCC fresh frozen samples was performed by the phenol-chloroform method. Ten µm sections from fresh-frozen tissues were cut and placed in 2mL eppendorfs, to which were added 500µL of SE buffer (75mM NaCl and 25 mM ethylenediamine tetraacetic acid EDTA), 30 µL of 10% SDS and 15µL of proteinase K [20mg/mL (NZYTECH, Portugal)] and the samples were incubated at 55ºC in agitation until DNA's digestion was complete. After this, 500µL of phenolchloroform solution at pH=8 (Sigma-Aldrich, USA) was added to Phase Lock Light tubes (5 Prime, Germany) and the samples were transferred to

the tubes. After this, the samples were centrifuged at 13000 rpm for 15min in order to separate the aqueous phase which contains the DNA. For the DNA precipitation, absolute ethanol (Merck, Germany) was added to it, in a proportion of two times the final volume of aqueous phase, as well as 7.5M Ammonium acetate (Sigma-Aldrich, Germany), in the proportion of one third of the final volume of aqueous phase. The samples were incubated overnight at -20°C. Then, the samples were centrifuged at 13000 rpm for 20min, and the pellets washed two times with 70% ethanol. Hence, the samples were centrifuged, and the pellets were dried at room temperature. Lastly, the DNA was eluted in sterile distilled water. For DNA concentration and purity ratio determination the NanoDrop Lite Spectrophotometer (Nanodrop Technologies, USA) was used.

VHL mutation status (VHL p.F76del c.226_228delTTC) was assessed using the QuantStudio™ 12K Flex Real-Time PCR System (Applied Biosystems, USA). For that, 100ng of DNA was mixed with 5ul of XpertFast Probe mix (GRiSP®, Porto, Portugal), 0,5ul of VHL probe (dHsaIS2505540, Bio-rad Laboratories, USA), at a final volume of 10ul per well in 384 well plates. All samples were run in triplicate and for each running a specific positive control was used. The following program was used: 1 cycle ate 95ºC for 3 minutes (polymerase activation), 45 cycles at 95ºC for 5 seconds (DNA denaturation) following 60ºC for 30 seconds (annealing and extension). Results were qualitatively evaluated and every sample with amplification was considered positive for this specific mutation.

4.4. RNA extraction, cDNA synthesis and quantitative reverse transcriptase polymerase chain reaction (qRT-PCR)

Total RNA was extracted using the ribozol reagent method. Ribozol (GriSP®, Porto, Portugal) was added to the cell pellets and these were homogenized mechanically with a pestle (VWR international, USA). After a 5min incubation at room temperature, the samples were transferred to RNase-free tube and chloroform (Merck, Germany) was added. Then, the samples were vortexed and incubated at room temperature for 3min. After being centrifuged at 13000rpm for 15min, the aqueous phase containing RNA was collected to new RNase-free tube. To precipitate the RNA, isopropanol (Merck, Germany) was added, and the samples were incubated at room temperature for 10min, and then centrifuged for another 10min at 13000rpm. Finally, the RNA pellets were washed two times using 75% ethanol and centrifuged two times for 5min at 13000rpm. After dried, the pellets were eluted in RNA storage solution (Invitrogen, USA). The RNA concentration and purity were assessed in NanoDropTM Lite Spectophotometer (Nanodrop Technologies, USA).

Synthesis of 1000 ng cDNA (DNA complementary) was accomplished by reverse transcription using RevertAid^{TM} RT Reverse Transcription Kit (ThermoScientific Inc, USA), according to the manufacturer procedures.

Quantitative reverse transcription polymerase chain reaction (qRT-PCR) was performed in 384-well plates LightCycler480II (Roche Diagnostics, Switzerland) using 450ng of diluted cDNA, 5µL of Xpert Fast SYBER Mastermix Blue (GRiSP®, Porto, Portugal) and 0.5µM of specific HIF-2α primers, at a final volume of 10µL per well. β-*GUS* was used as a housekeeping gene to normalize HIF-2α expression in our selected cohort. All the samples were run in triplicates. The relative HIF-2α transcript levels were calculated as the ratio between the HIF2α mean quantity and β-*GUS* mean quantity (Gene Expression Level = Gene Mean Quantity / β-GUS Mean Quantity).

4.5. MCTs knockdown: CRISPR/Cas9 technology

In order to evaluate the impact of MCTs inhibition on cell survival and tumour aggressiveness, MCTs silencing was performed through CRISPcas9 technology. For that we resorted to a plasmid with a specific guide RNA sequence (GenScript, Piscataway, NJ, USA), targeting MCT1 (*SLC16A1* seq: CGTATAGTCATGATTGTTGGTGG) and MCT4 (*SLC16A3* seq: TTCGGCTGTTTCGTCATCACTGG) isoforms, respectively. In parallel, scramble vector targeting a nonspecific guide RNA sequence (GenScript, Piscataway, NJ, USA) was used. After 5x10^4 ccRCC cells (Caki1, 769P and 786-O) seeding, 500ng plasmid-guide RNA vector (GenScript Piscataway, NJ, USA) transfection with Lipofectamin 3000 (Invitrogen, USA) was performed in RPMI medium without FBS and 1% penicillin/streptomycin, overnight. Then, selection of puromycin resistant cells was performed, whose ideal concentration was determined by a puromycin calibration curve, obtaining 0.5 µg/ml puromycin for Caki-1 and 1 µg/ml puromycin for 786-O and 769-P cell lines. Then, to obtain a higher MCTs downregulation, a limit dilution assay for clone selection was performed.

For the clone selection, 4000 cells of each cell line were seeded in the first well of a 96-well plate following a serial dilution throughout the entire plate (1:2 ratio in the vertical direction followed to 1:2 ratio in the horizontal direction). The wells with fewer cells were identified and after their expansion, RNA was extracted to assess MCTs transcript levels. MCTs silencing was confirmed through western blot (WB).

4.6. Western blot

Total protein was extracted from Caki-1, 769-P and 786-O cells lines at basal levels, as well as from MCT1 and MCT4 silenced conditions. Cells were collected from the culture flasks, homogenized in RIPA lysis buffer (Santa Cruz Biotechnology, USA) supplemented with proteases inhibitors cocktail (Sigma-Aldrich, Germany). After that, the samples were incubated 15min in ice following centrifuge at 13300 rpm for 30min at 4ºC. The supernatant was collected, and the Pierce BCA Protein Assay Kit (Thermo Scientific Inc, USA) was used to measure the protein levels, according to the manufacture's procedures. The protein's concentration was determined using a calibration curve. Then, 20 µg of total protein was separated in 10% polyacrylamide gel by sodium dodecyl sulphate polyacrylamide gel electrophoresis (SDS-PAGE) and transferred into an immunoblot nitrocellulose membrane (Bio-Rad Laboratories, USA) in a Tris-base/ glycine buffer using a Transblot Turbo Transfer system (Bio-Rad Laboratories, USA). To do the immunoblotting, membranes were blocked with 5% milk in tris-buffer saline/0.1% Tween (TBS-T; pH=7.6) for 1h at room temperature. Hereafter, the membranes were incubated overnight at 4ºC with the specific primary antibodies (Table 3). After incubation, the membranes were washed in TBS-T and incubated with secondary antibody attached with horseradish peroxidase (1:5000, Cell Signalling Technology, USA) for 1h at room temperature. Lastly, membranes were washed with TBS/T and exposed into Clarity WB ECL substrate (Bio-Rad Laboratories, USA) using the ChemiDoc Imaging System (Bio-Rad Laboratories, USA). Western blot quantification results using band densitometry analysis was performed using ImageJ software (version 1.41, National Institute of Health (NHI)). β-ACT was used to loading control.

Table 3. Antibodies used in Western Blot and respective dilutions.

Primary antibody	Company	Dilution	Second antibody specie
VHL	Cell Signalling Technology, #685475	1:1000	Anti-rabbit
HIF-1α	Cell Signalling Technology, #361695	1:250	Anti-rabbit
HIF-2α	Abcam, ab243861	1:500	Anti-rabbit
MCT1	Santa Cruz Biotechnology, sc-365501	1:250	Anti-mouse
MCT4	Santa Cruz Biotechnology, sc-376140	1:250	Anti-mouse
GLUT-1	Cell Signalling Technology, #129395	1:250	Anti-rabbit
HKII	Cell Signalling, Technology #28675	1:250	Anti-rabbit
LDHA	Cell Signalling Technology, #35825	1:1000	Anti-rabbit
PKM2	Cell Signalling Technology, #40535	1:1000	Anti-rabbit
β-catenin	Cell signalling Technology, #8480	1:1000	Anti-rabbit
Vimentin	Cell signalling Technology, #5741	1:1000	Anti-rabbit
β-actin	Sigma-Aldrich, A1978	1:10000	Anti-mouse

4.7. Immunofluorescence

Immunofluorescence (IF) was performed to assess the protein expression and cellular localization of MCT1 and MCT4, as well as hypoxic related metabolic markers, such as LDHA, PKM2, GLUT-1, HKII, HIF-1α and HIF-2α, in all MCT1 and MCT4 downregulated ccRCC cell lines. The cells were seeded in 96 well plates at 2500 cells/well density, overnight. Briefly, cells were fixed 10min in 4% paraformaldehyde (PFA, Santa Cruz Biotechnology, USA) or methanol (Merck, Germany), following cell permeabilization with Triton™ X-100 0.25% or 0.50% in 1x phosphate-buffer saline (PBS) during 15 min (Table 4). After, cells were blocked with 5% bovine serum albumin (BSA, Thermo Fischer Scientific, USA) in 1x PBS, for 30min and incubated with primary antibodies (Table 4), overnight at room temperature. In the next day, cells were incubated with secondary antibody anti-mouse immunoglobulin G (IgG) tetramethylrhodamine (TRITC) (Alexa Flour™ 594, 1:500, A11005, Invitrogen, USA) or anti-rabbit IgG-fluorescein isothiocyanate (FITC) (Alexa Fluor™ 488, 1:500, A11008; Invitrogen, USA), for 1h at room temperature. Then, cells were stained with 4',6- diamidino-2-phenylindole (DAPI; 1:20 dilution; AR1176, BOSTER Biological Technologies, China). Pictures were taken in a fluorescence microscope Olympus IX51 with a digital camera Olympus XM10 using CellSens software (Olympus, Japan) (200x magnification).

Table 4. Antibodies used in the immunofluorescence with fixation and permeabilization methods, respectively.

Primary antibody	Company	Dilution	Fixation	Permeabilization	Second antibody specie
HIF-1α	Cell Signalling Technology, #361695	1:250	PFA (4%)	Triton™ X-100 0.5%	Anti-Rabbit
HIF-2α	Abcam, ab243861	1:200	PFA (4%)	Triton™ X-100 0.5%	Anti-Rabbit
MCT1	Santa Cruz Biotechnology, sc-365501	1:100	Methanol	-------	Anti-mouse
MCT4	Santa Cruz Biotechnology, sc-376140	1:500	Methanol	-------	Anti-mouse
GLUT-1	Cell Signalling Technology, #129395	1:250	Methanol	-------	Anti-Rabbit
HKII	Cell Signalling Technology, #28675	1:100	PFA (4%)	Triton™ X-100 0.25%	Anti-Rabbit
LDHA	Cell Signalling Technology, #35825	1:500	Methanol	Triton™ X-100 0.5%	Anti-Rabbit

PKM2	Cell Signalling Technology, #40535	1:500	PFA (4%)	Triton™ X-100 0.25%	Anti-Rabbit

4.8. Metabolism assay

To assess the impact of MCTs downregulation in the cellular metabolism, particularly in the glycolytic activity of our studied ccRCC cell lines, glucose consumption and lactate production were measured. Scramble and MCTs downregulated ccRCC cell lines (786-O and 769-P, $2x10^4$ cells/ well (500µl) and Caki-1, $4x10^4$ cells/well, respectively) were seeded and allowed to growth overnight in RPMI complete culture medium at 37ºC. Then, RPMI completed culture medium was removed and ccRCC cell lines were incubated with RPMI culture medium without FBS. Cell culture medium (50µl) was collected after 24, 48 and 72 hours and stored at -20ºC until glucose and lactate quantification. In these time points, cell growth was assessed using the MTT ((3-(4,5-dimethylthiazol-2-yl)-2,5-diphenyltetrazolium bromide) assay (Sigma-Aldrich, Germany). Results represent, at least four independent experiments, each one in triplicates. Glucose consumption and lactate production were expressed as total [g/L]/cell growth and total [mM]/cell growth, respectively.

Extracellular Glucose Quantification

Extracellular glucose content was assessed by an enzymatic colorimetric kit (Spinreact, Spain), based on the enzymatic oxidation of glucose by glucose-oxidase (GOD) to gluconolactone and hydrogen peroxide (H_2O_2). The formed H_2O_2 is detected by a chromogenic oxygen acceptor, phenol, 4-aminophenazone (4-AP) in the presence of peroxidase (POD), converting in a quinone compound suitable for spectrophotometric quantification. The colour intensity of the compound formed is directly proportional to the glucose concentration in the sample:

$$\beta\text{-D-Glucose} + O_2 + H_2O \rightarrow \text{Gluconid acid} + H_2O_2$$

$$H_2O_2 + \text{Phenol} + \text{4-AP} \rightarrow \text{Quinone} + H_2O_2$$

Briefly, 2µl of each sample was mixed with 100µl of working solution and incubated for 20min at room temperature in the dark. Blank was performing by adding 100µl of working solution. The absorbance was read at 490nm in a microplate reader (Fluostar Omega, BMG Labtech). Calculation of glucose levels was based on a calibration curve with a range of glucose concentrations.

Extracellular Lactate Quantification

The extracellular lactate levels were assessed using a colorimetric kit (Spinreact, Spain), where lactate is oxidized to pyruvate and H_2O_2, by lactate oxidase (LO). Then, H_2O_2 is metabolized by peroxidase (POD) and converted into quinone, a red compound from whom the intensity of the colour is directly proportional to the lactate concentration in the sample:

$$\text{L-Lactate} + O_2 + H_2O \rightarrow \text{Pyruvate} + H_2O_2$$

$$\text{L-}2H_2O_2 + \text{4-AP} + \text{4-Chrolophenol} \rightarrow \text{Quinone} + H_2O$$

Briefly, 200µl of working solution was mixed with 2µl of each sample and incubated for 10min at room temperature in the dark. Blank contained 200µl of working solution alone. The absorbance was read at 490nm in a microplate reader (Fluostar Omega, BMG Labtech). Calculation of lactate levels was based in a calibration curve with a range of lactate concentrations.

4.9. Trypan blue dye exclusion assay

Trypan blue assay is a dye exclusion test used to determine the number of viable cells presented in a cell suspension. It is based on the principle that live cells possess intact cell membranes that exclude trypan blue, whereas dead cells do not. In this test, a cell suspension is simply mixed with dye and then visually examined to determine whether cells take up or exclude dye. Thus, viable cells have a clear cytoplasm whereas a nonviable cell will have a blue cytoplasm.

Briefly, Caki-1, 769-P and 786-O cells were plated into 24-well plates, at a density of $1x10^4$ cells per well and allowed to adhere overnight in complete RPMI medium. After 72h, cells were washed with 200µl PBS, followed to 100µl trypsin incubation during 5min at 37ºC. Behind, trypsin inactivation, cells were collected and a mix of 10µl cells + 10µl of 0.4% trypan blue was prepared for viable cell count in Neubauer Chamber. The results represent the mean±SD of six independent experiments, each one in triplicates, and normalized for the scramble condition.

4.10. Colony formation assay

ccRCC cells for scramble and MCTs downregulation conditions were seeded in 6-well plates at a density of 500 cells per well. After 5 days, upon colony formation, cell colonies were washed with 1xPBS, fixed with methanol (Merck, Germany) for 10 min and washed again with 1xPBS. Cell colonies were incubated with crystal violet solution for 1 min,

followed by washing with 1xPBS. Finally, cells were washed with distillate water for 2 min and left to dry overnight. Colonies (≥20 cells) were counted using an Olympus SXZ16 stereomicroscope. The survival fraction (SF) was calculated according to the following formula SF = [number of colonies / (number of plated cells * platting efficiency (PE))], where PE is calculated according to PE= (number of colonies counted / number of plated cells). The results are representative of at least four independent experiments and normalized for the scramble condition.

4.11. Proliferation assay

Cell proliferation was measured using the BrdU cell proliferation Kit (BioLegend Inc., USA). In this assay 5-bromo-2'-deoxyuridine (BrdU), a pyrimidine analog, is incorporated in place of pyrimidine into the newly synthesized DNA. The quantity of BrdU incorporated into cells is directly correlated to the number of proliferating cells. Caki-1, 769-P, and 786-O cells for MCT1 and MCT4 knockdown were plated into 6-well plates, at a density of $1x10^5$ cells per well and allowed to grow in complete RPMI medium during 48h. Later, the cells were harvested, loaded with 5µg/mL BrdU solution during 1h30min at 37ºC. Afterwards, cells were centrifuged for 5min at 1200rpm washed with 200µl of Cell Staining Buffer. After centrifuging at 2100rpm for 2min, cells were fixed during 20min at 4ºC, followed cell permeabilization during 10 min at room temperature. Subsequently, cells were washed and fixed again. before the treatment with 25µl of DNAse at 37ºC for 1h. Then, cell staining with anti-BrdU antibody (2.5µl of anti-BrdU antibody in 45µl of cell staining buffer) was performed for 20min at room temperature in the dark. Cells were washed and stained with 7-aminoactinomycin D (7-AAD) during 10min prior to cell acquisition on a flow cytometer FACS CantoTM II Cell Analyzer (BD Biosciences, USA). Flow cytometry analysis was carried out using FlowJoTM software (BD Biosciences, USA). Results are representative at least of three independent experiments.

4.12. Invasion assay

Cell invasion was evaluated by using 24-well BD BioCoat Matrigel Invasion Chambers, with 8µm pore size membranes (BD BioSciences, USA). These invasion chambers allow to compare the *in vitro* cells invasive behaviour: the thin layer of Matrigel Matrix mimics a basal membrane that occludes the pores of the membrane, blocking non-invasive cells from migrating through the membrane. In contrast, invasive cells are able to dethatch themselves and invade through the Matrigel Matrix and the 8µm membrane pore. Firstly, Matrigel Matrix Chambers were rehydrated with serum free culture medium for 1h30min at 37ºC, 5% CO_2

atmosphere. After rehydration, the medium was removed and 500µl of cell culture medium with 10% FBS was added into the well. Then, $2x10^4$ Caki-1 cells/insert and $1.5x10^4$ 769-P and 786-O cells/insert in serum free medium were seeded in the insert and incubated at 37ºC in 5% CO_2. After 24h, non-invading cells were removed from the upper surface of the membrane with a swab, and invading cells in the lower surface of the membrane were fixed with cold methanol for 20min and stained with crystal violet solution (Active Motif Inc., USA) during 10min, following by washing in 1x PBS 3 times for 2 min. Membranes were photographed in Olympus SZX16 stereomicroscope with a digital camera system (Olympus SC180). Invading cells were counted using the Image J software (version 1.41, NIH) and invasion was calculated as % of cell invasion normalized for the scramble condition. Results are the mean±SD of four independent experiments.

4.13. Wound-healing assay

The wound-healing assay is one of the earliest developed methods to study directional *in vitro* cell migration. The principle is based on creating a "wound" in a cell monolayer, capturing images at regular intervals until wound closure, and comparing the images to quantify the cells' migration rates. $1x10^6$ cells of 769-P, 786-O and Caki-1 cells were seeded in 6-well plates and allowed to reach confluence at 37ºC and 5% CO_2 for 24 hours. Then, two "wounds" was made by manual scratching with a 200µL pipette tip and cells were gently washed with 1X PBS in order to remove detached cells in the wound. Then cells were incubated with freshly RPMIc medium and the ''wounded'' areas were photographed in four specific wound sites at 40x magnification using a Olympus IX51 inverted microscope equipped with a Olympus XM10 Digital Camera System at 0, 6, 12 and 24 hours. The relative migration distance (5 measures by wound) was calculated with the following formula:

$$\text{Relative migration distance (\%)} = (A–B)/C \times 100$$

where A is the width of cell wound at 0h of incubation, B is the width of cell wound after a specific hour of incubation, and C is the width mean of cell wound to the at 0h of incubation. For relative migration distance, the results were analyzed using the beWound—Cell Migration Tool (Version 1.5) (developed by A.H.J. Moreira, S. Queirós and J.L. Vilaça, Biomedical Engineering Solutions Research Group, Life and Health Sciences Research Institute- University of Minho; available at http://www.besurg.com/sites/default/files/beWoundApp.zip). At least three independent experiments were conducted.

4.14. Chorioallantoic membrane (CAM) assay

Fresh fertilized eggs (PintoBar, Lda, Portugal) were incubated at 37°C in a humid environment. After 3 days of embryonic development, a window was opened into the eggshell under aseptic conditions to check embryo viability and return to incubator. On day 13, $2x10^6$ of 769-P, 786-O and Caki-1 scramble and MCTs knockdown cells in 25uL of BD Matrigel™ Matrix Growth Factor Reduced (BD Biosciences) were seeded on the CAM. On day 17, *in ovo* and the *ex ovo* microtumour images were obtained using the stereomicroscope Olympus SZX16 with a digital camera Olympus SC180.

4.15. Statistical analysis

Statistical analysis was performed using the GraphPad Prim 6.0 software (GraphPad Software Inc., USA). Non-parametric Mann-Whitney U test was used to compare two groups, while Kruskall-Wallis test was used for multiple groups, followed by Dunn's multiple comparison test for pairwise comparisons. P-values were considered statistically significant when inferior to 0.05. Significance is shown vs. the respective control and depicted as follows: *p<0.05; **p<0.01; ***p<0.001; ****p<0.0001 and ^{ns}p>0.05 (non-significant).

RESULTS

5.1. VHL status characterization in ccRCC

In order to characterize *VHL* mutation status in the available cohort, an assay for one of the most evaluated mutation (VHL p.F76del c.226_228delTTC) was used. In a series of 200 patients, this specific deletion was found only in 4% of them (Table 5).

Table 5. Percentage of ccRCC positive cases for the specific VHL mutation "p.F76del c.226_228delTTC".

Mutation: VHL p.F76del c.226_228delTTC	Positive	Negative
Patients	8	192

5.2. HIF-2α was upregulated in ccRCC patients' samples

The transcription factor HIF-1α is known to be important in tumour cell metabolism reprogramming. Previously in our group, HIF-1α expression was characterized in the ccRCC cohort. Unlike expected, at transcriptional levels, a significant decrease on HIF-1α expression in ccRCC samples compared to normal kidney samples was observed (preliminary results). However, the IHC analysis showed a significantly increase in HIF-1α nuclear expression for ccRCC tissues compared normal kidney ($p<0.0001$, 73% (163/223) vs 0% (0/30), respectively). Since most cancers rely on HIF-1α to mediate tumour metabolism [91] but a decreased was previously observed in ccRCC transcript levels, HIF-2α relative expression levels were assessed this time. In fact, HIF-2α has been shown to be involved in ccRCC carcinogenesis and the transcript levels were higher in our ccRCC samples when compared to normal kidney, as shown in figure 13A. Sadly, IHC analysis could not be obtained for HIF-2α once we were not able to optimize the commercially available antibodies. Despite these results, a positive correlation between HIF-1α expression and tumour grade was found, showing HIF-1α higher levels in more advanced stages of the disease (Figure 13B). However, there was no correlation between HIF-2α expression levels and tumour grade (Figure 13C).

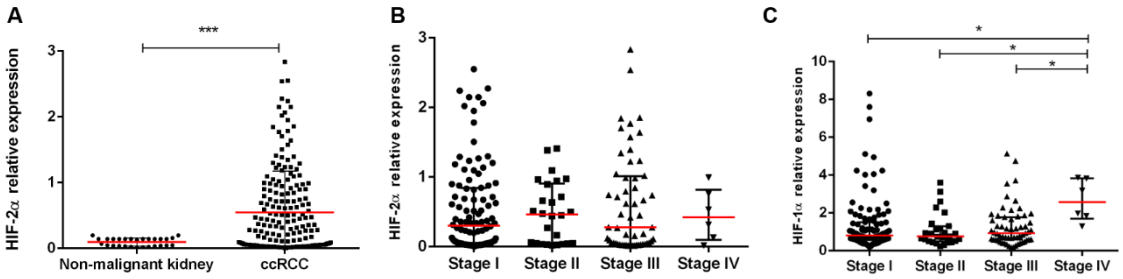

Figure 13. HIF-2α expression was upregulated in ccRCC and HIF-1α expression increases with disease stage. HIF-2α transcript levels evaluated through qRT-PCR in ccRCC and normal kidney samples **(A)**. HIF-1α **(B)** and HIF-2α **(C)** relative expression in the four grades of ccRCC. Each sample was run in triplicates. *p<0.05; ***p<0.001.

5.3. Glycolytic and hypoxia markers were differently expressed in ccRCC lines

On a first approach, glycolytic and hypoxia related markers were evaluated in the three ccRCC cell lines (Caki-1, 769-P and 786-O) with different VHL status (Figure 14). This was confirmed through WB, where the only cell line expressing the VHL protein was Caki-1 (Figure 14). As expected, Caki-1 expressed lower MCTs protein levels than 769-P and 786-O. Furthermore, 769-P expressed higher MCT4 levels whereas 786-O presented higher MCT1 levels (Figure 14). Regarding the hypoxia markers, 769-P and 786-O expressed higher HIF-1α and HIF-2α, levels than Caki-1. Notably, HIF-2α expression, but not HIF-1α, was slightly augmented in 786-O when compared to 769-P (Figure 14). Other important glycolytic markers, such as GLUT1, HKII, LDHA, PDK and PKM2, were also evaluated, having been observed an increase in all of them for 769-P and 786-O compared to Caki-1, except PKM2 whose expression did not vary between the three cell lines, as well as LDHA expression between Caki-1 and 769-P cell lines (Figure 14).

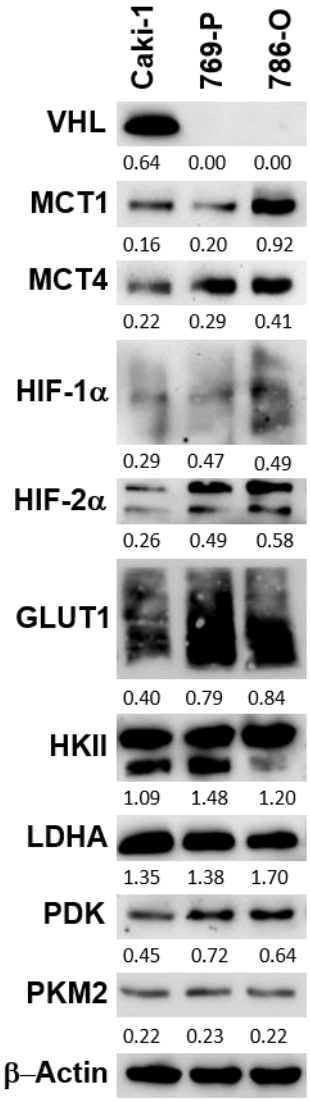

Figure 14. Characterization of MCTs and hypoxia-related metabolic markers expression in ccRCC cell lines by Western Blot. Results are representative of 3 independent replicates. Molecular weights: VHL: 20kDa, MCT1: 45kDa, MCT4: 43kDa, HIF-1α: 120kDa, HIF-2α: 115kDa, GLUT1: 45-60kDa, HK2: 102kDa, LDHA: 37kDa, PDK: 47kDa, PKM2: 60kDa and β-actin: 42kDa.

5.4. MCTs downregulation affected glycolytic metabolism, decreasing the lactate production

Taking into consideration MTCs role in cancer cells metabolism and its upregulation in different tumour types [44], as shown previously in our group for ccRCC (preliminary results), studying how MCTs downregulation could affect tumour aggressiveness, particularly in ccRCC, was of our interest. This way, a CRISPR/cas9-mediated MCTs knockdown/knockout was performed in ccRCC cell lines. The knockdown was confirmed

through WB (Figure 15A) and IF (Figure 15B-D) for the different clones obtained for each cell line, respectively. 769-P MCT1 B11 clone only presented a silencing percentage of 15%, whilst the other two clones, MCT1 F7 and MCT1 H3, presented 90% and 80%, respectively (Figure 15A). Surprisingly, almost all 769-P clones, even the ones silenced for MCT1, presented silencing above 98% for MCT4 (Figure 15B). On the other hand, MCT4 B7 expressed 0.28 protein levels for MCT4, which was also verified by IF in figure 15B. In 786-O cell line, MCT1 D7 and MCT1 H3 had lower protein levels compared to the scramble condition, with silencing percentages of 46% and 74%, which correlated with the decreased MCT1 expression in the cell membrane (Figure 15C). The same happened for MCT4 F5 and MCT4 G2 clone, which showed similar silencing, 74% and 76%, respectively (Figure 15A). This was also confirmed in the IF panel where a decrease in MTC4 cell membrane expression was observed for these clones (Figure 15C). Notwithstanding, 786-O clones silenced for MCT1 express MCT4, and vice versa, with MCT1 D7 and MCT1 H3 having a silencing percentage of 65 and 37% for MCT4, and MCT4 F5 and MCT4 G2, expressing 56 and 70% of MCT1 cells (Figure 15A). Finally, Caki-1 MCT1 A6 and D9 clones showed 95 and 78% of silencing and no differences were observed, nor at protein levels nor in the IF, for MCT4 in these two clones (Figure 15A and D). In addition, MCT4 C5 and H3 clones presented a silencing percentage of 45% and 77% for MCT4 levels, having been observed 13 and 2% of cells with MCT1 levels, respectively (Figure 15A).

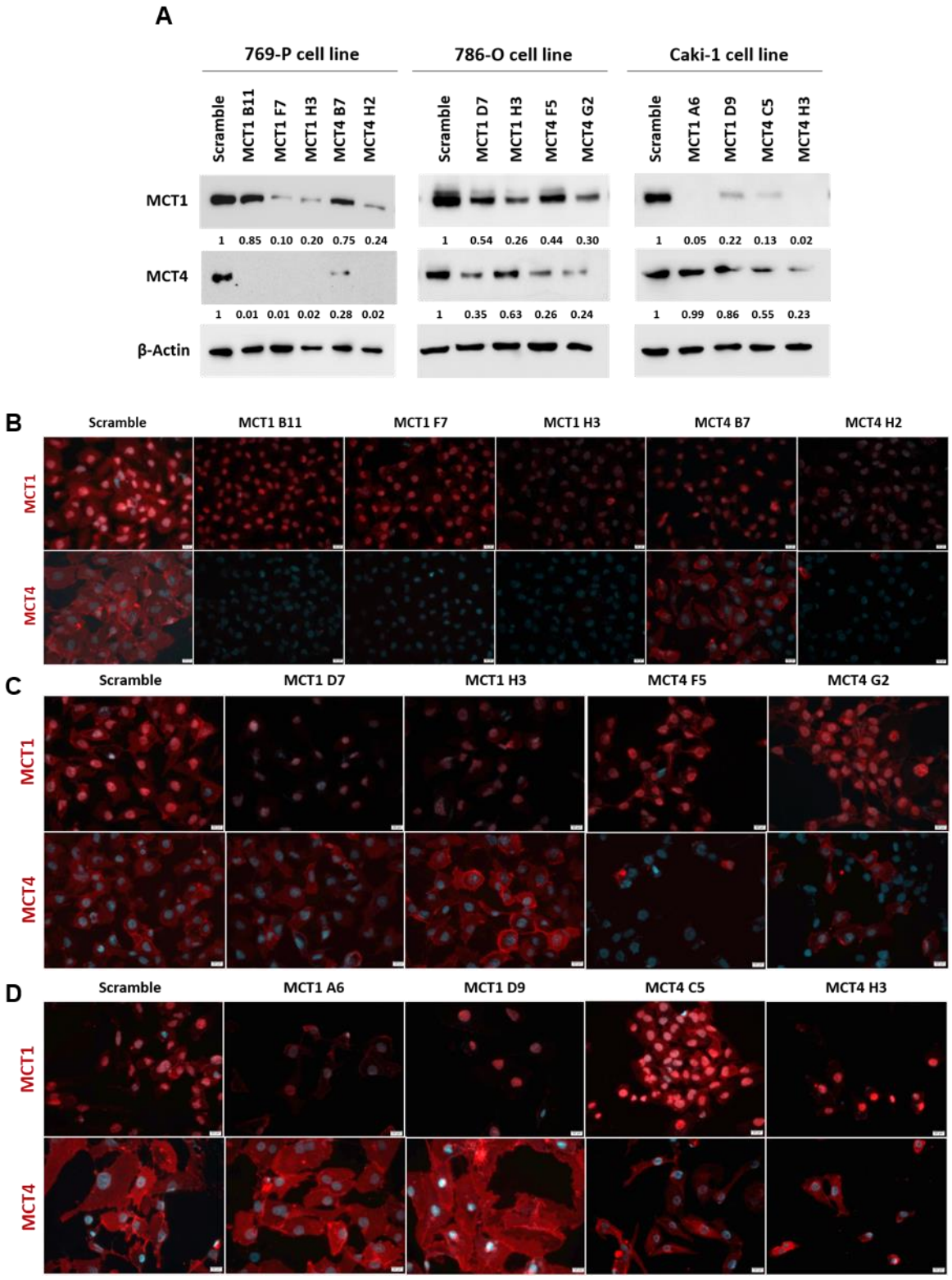

Figure 15. MCTs were downregulated in different ccRCC cells after CRISPR/cas9 transfection. CRISPR/Cas9-mediated MCTs knockdown in the obtained clones was confirmed by WB **(A)** and IF for ccRCC cell lines 769-P **(B)**, 786-O **(C)** and Caki-1 **(D)**. Results are representative of three independent replicates. Molecular weights: MCT1: 45kDa, MCT4: 43kDa and β-actin: 42kDa.

Considering MCTs engagement in the glycolic pathway, the effect of MCT1 and MCT4 knockdown was further confirmed through glucose consumption (Figure 16A) and lactate production evaluation (Figure 16B). Glucose consumption was lower for all MCT1 and MCT4 clones in the three cell lines, being significantly decreased in 769-P MCT1 H3 and MCT4 H2 and in 786-O MCT4 clones (Figure 16A). Despite the decrease observed in Caki-1, no statistically differences were found between the MCT knockdown clones and the scramble condition. However, lactate production was significantly lower in all MCTs clones, except for Caki-1 MCT1 A6 and D9, with a clear decrease in 769-P MCT4 H2, 786-O MCT4 G2 and Caki-1 MCT4 C5 and H3 clones (Figure 16B).

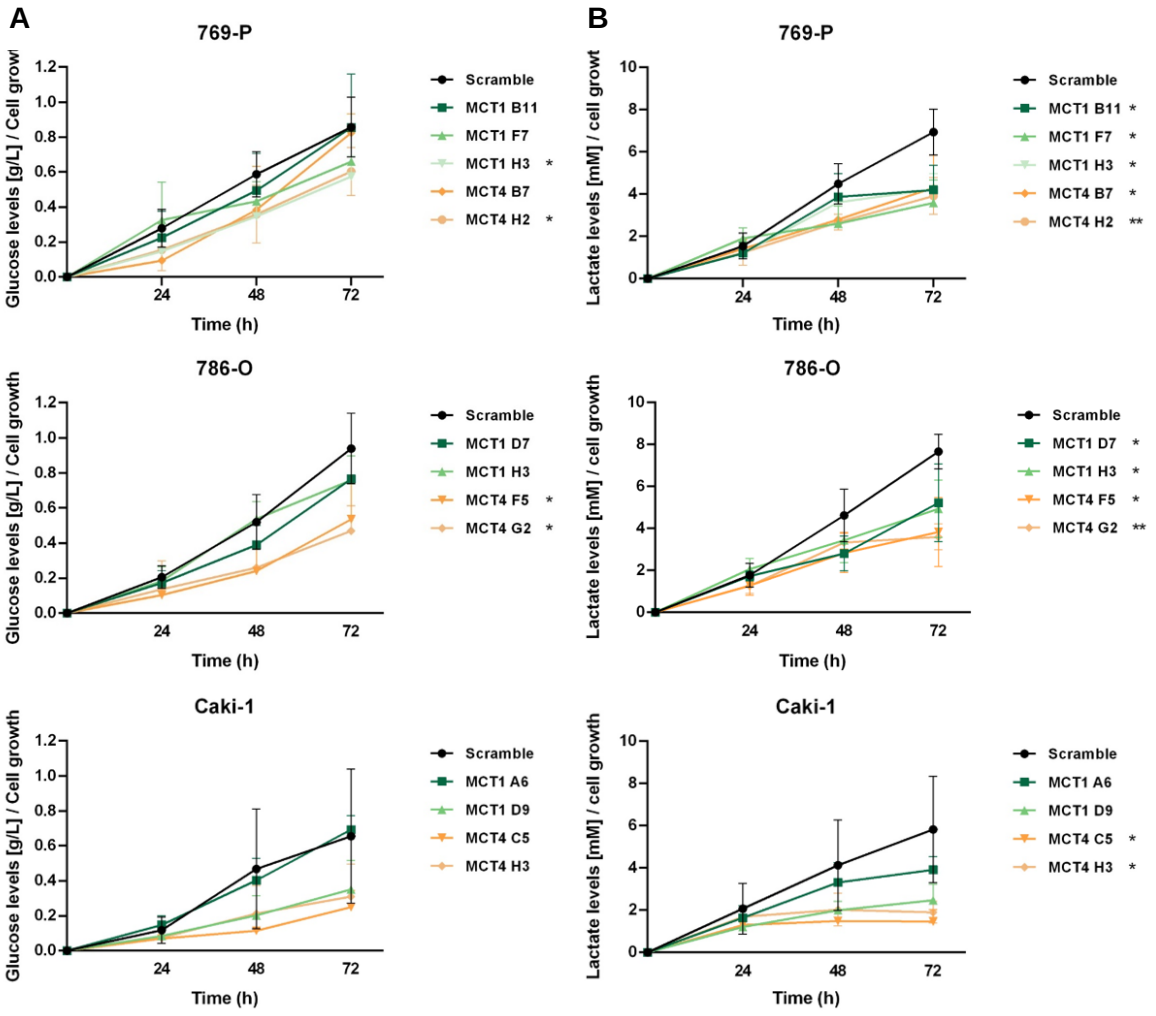

Figure 16. MCTs knockdown decreased glucose consumption and lactate production in ccRCC. Glucose consumption **(A)** and lactate production **(B)**, over time, in the different MCTs knockdown clones obtained for each ccRCC cell line 769-P, 786-O and Caki-1. Results are the mean of, at least, four independent replicates, each one in triplicates. *p<0.05; **p<0.01 for specific MCTs knockdown clone compared to scramble.

5.5. MCTs knockdown altered the HIF-related glycolytic phenotype in ccRCC cells

After MCTs knockdown confirmation, the obtained clones where characterized for different metabolic markers through WB (Figure 17A) and IF (Figure 17B). In 769-P cell line, GLUT1 expression decreased in all the clones, excepting MCT1 B11 clone, both in the WB and in the IF. The same happened in Caki-1 cell line, with GLUT1 being almost absent in MCT4 clones. In 786-O cell line, the difference was not so apparent, with MCT1 D7 clone presenting higher GLUT1 levels both in WB and IF.

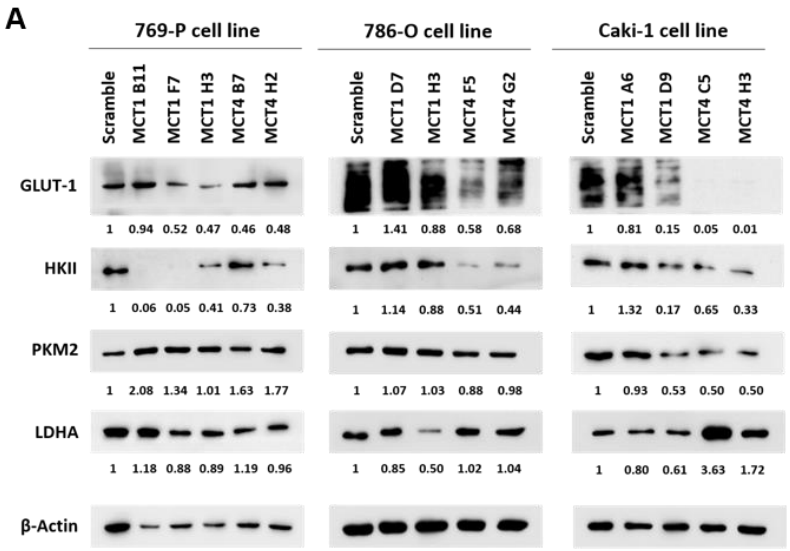

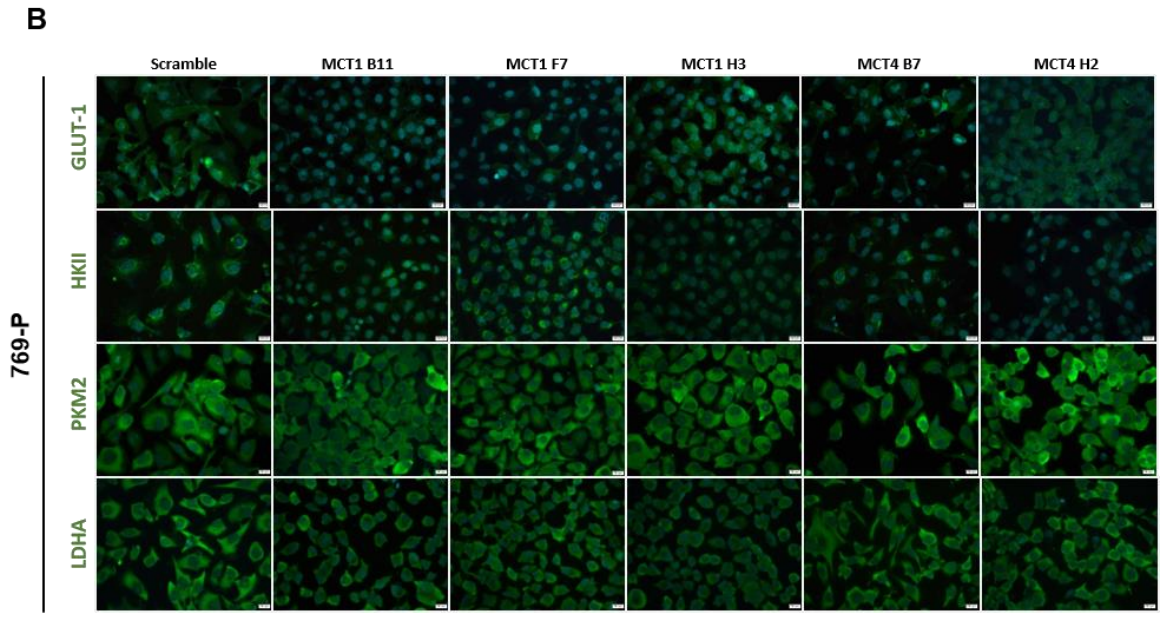

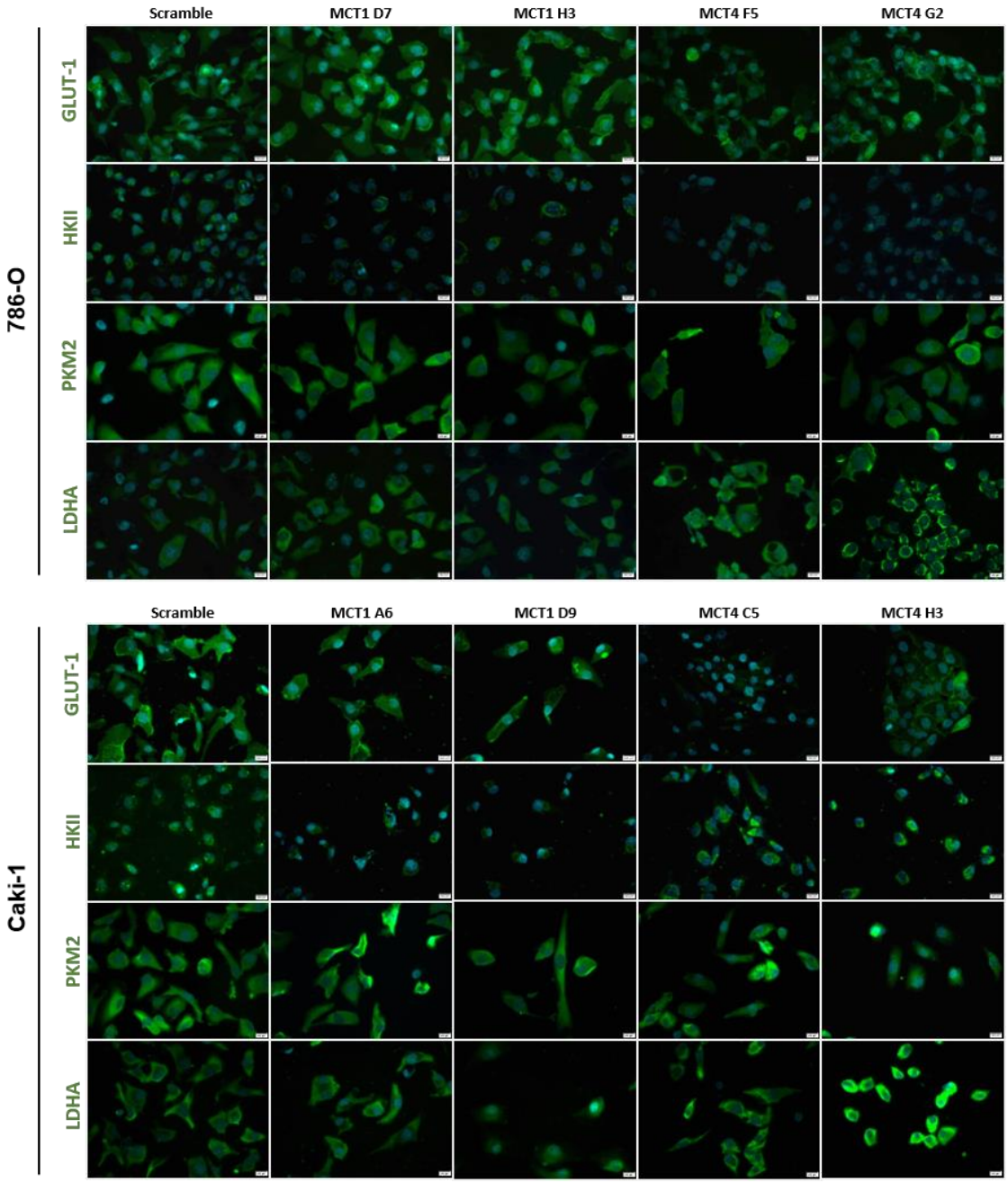

Figure 17. MCT1 and MCT4 knockdown showed differential metabolic markers expression in ccRCC cells. Characterization of metabolic markers expression by WB **(A)** and IF **(B).** Results are representative of three independent replicates. Molecular weights: GLUT1: 45-60kDa, HKII: 102kDa, LDHA: 37kDa, PKM2: 60kDa and β-actin: 42kDa**.**

Despite HKII protein levels being absent in 769-P MCT1 B11 and F7 clones (Figure 17A), its presence was still observed in the IF (Figure 17B), although in lower levels than the scramble condition. All the other 769-P MCTs knockdown clones showed lower levels of HKII, both in the WB and IF. For 786-O cell line, MCT1 clones displayed similar HKII protein levels when compared to the scramble condition. However, the contrary happened for 786-

O MCT4 clones, where we could observe a decrease to roughly half of HKII protein levels in WB and almost no expression in the IF (Figure 17A and B). HKII levels were significantly lower for all Caki-1 MCTs knockdown clones, excepting MCT1 A6, when compared to the scramble (Figure 17A and B). Furthermore, PKM2 protein levels showed little to no difference for 769-P and 786-O cell lines in the WB and IF. However, a decrease was observed for Caki-1 cell line, particularly in MCT4 clones (Figure 17A and B). 769-P and 786-O MCT1 clones, excepting 769-P MCT1 B11, presented a slight reduction in LDHA protein levels whilst no alterations were observed for MCT4 clones, both in the WB and IF (Figure 17A and B). LDHA expression decreased in both Caki-1 MCT1 clones, showing highly increased levels for Caki-1 MCT4 clones, both in WB and IF (Figure 17A and B). Concerning the hypoxia inducible factors, HIF-1α and HIF-2α, in Figure 18, one could observe a decrease in its nuclear levels in 769-P MCTs downregulation clones, specifically HIF-1α abrogation for MCT1 knockdown comparativly to the scramble condition. Furthemore, HIF-1α staining levels were decreased in 786-O and Caki-1 cells for both MCT4 knockdown clones (Figure 18). In addition, no significant effect was observed in all 786-O and Caki-1 MCTs knockdown clones concerning HIF-2α nuclear staining levels (Figure 18).

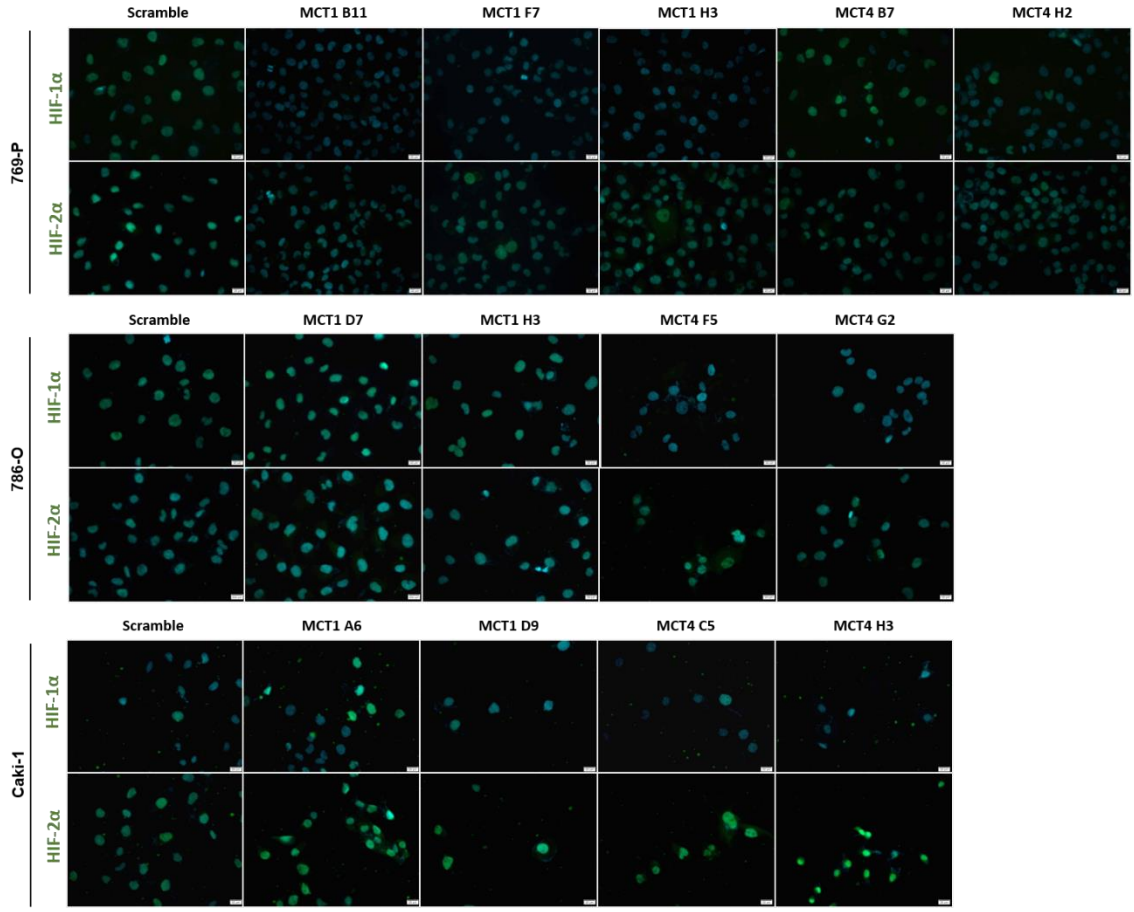

Figure 18. HIF-1α and HIF-2α profile for MCT1 and MCT4 knockdown in ccRCC cells. Characterization of hypoxic markers expression by IF**.** Pictures were taken in a fluorescence microscope (Olympus IX51) with a digital camera (Olympus IX81) at 400x magnification.

5.6. MCTs inhibition' affected tumour growth and proliferation

After the metabolic characterization, it was of our interest to evaluate the *in vitro* impact of MCTs inhibition on tumour aggressiveness. In fact, ccRCC-MCTs knockdown cells displayed a significant decrease in cell growth when compared to the scramble condition (Figure 19A), predominantly 768-O and Caki-1 cell lines. Contrarily, 769-P MCT1 B11 cell growth was higher than the scramble condition. Similarly, the clonogenic capacity of ccRCC-MCTs knockdown cells was significantly lower for all clones except for 769-P MCT1 B11 and Caki-1 MCT1 A6, where a decrease can be observed despite not being statistically significant (Figure 19B). Furthermore, in Caki-1 cell line the decrease in colony formation was more pronounced in MCT4 clones.

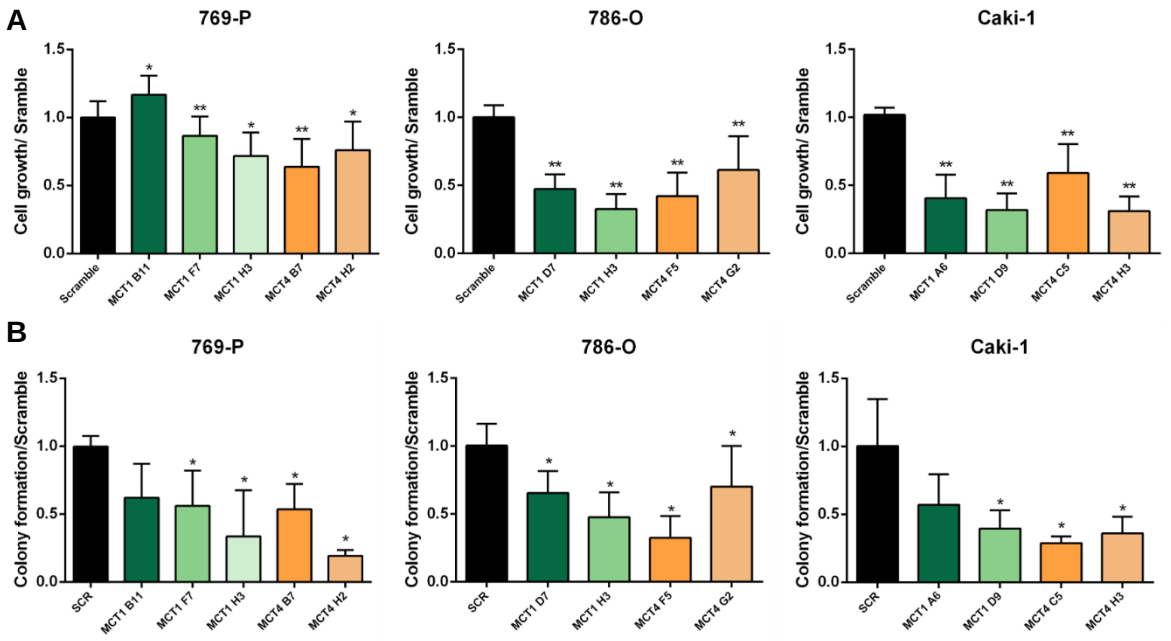

Figure 19. MCTs downregulation promoted decreased cell growth and colony formation in ccRCC. MCTs knockdown effect on tumour growth by Trypan blue dye exclusion assay **(A)** and on the clonogenic capacity **(B)** of ccRCC cells. Results are compared to scramble condition and represents the mean of, at least, five independent experiments. *p<0.05; **p<0.01 for specific MCTs knockdown clone compared to scramble.

Regarding cell proliferation, BrdU incorporation into MCTs-knockdown cells was lower than the scramble condition in all cell lines (Figure 20), although only statistically significant in Caki-1 MCT1 A6, MCT1 D9 and MCT4 C5 clones. Interestingly, the cells' percentage in the S phase of the cell cycle was lower for 769-P MCT1-knockdown clones but the contrary happened in 786-O, where MCT4-knockdown clones showed a decreased percentage of cells in the S phase compared to the scramble condition (Figure 20A and B). However, all Caki-1 clones showed a decrease in BrdU cell incorporation, namely a decrease in the S phase of the cell cycle, with no emphasis in a specific MCT isoform. In addition, for Caki-1 MCT1 knockdown clones an increase on G2/M phase was observed (Figure 20A). Moreover, for 769-P and 786-O MCTs knockdown clones an increase on G0-G1 phases was observed (Figure 20A).

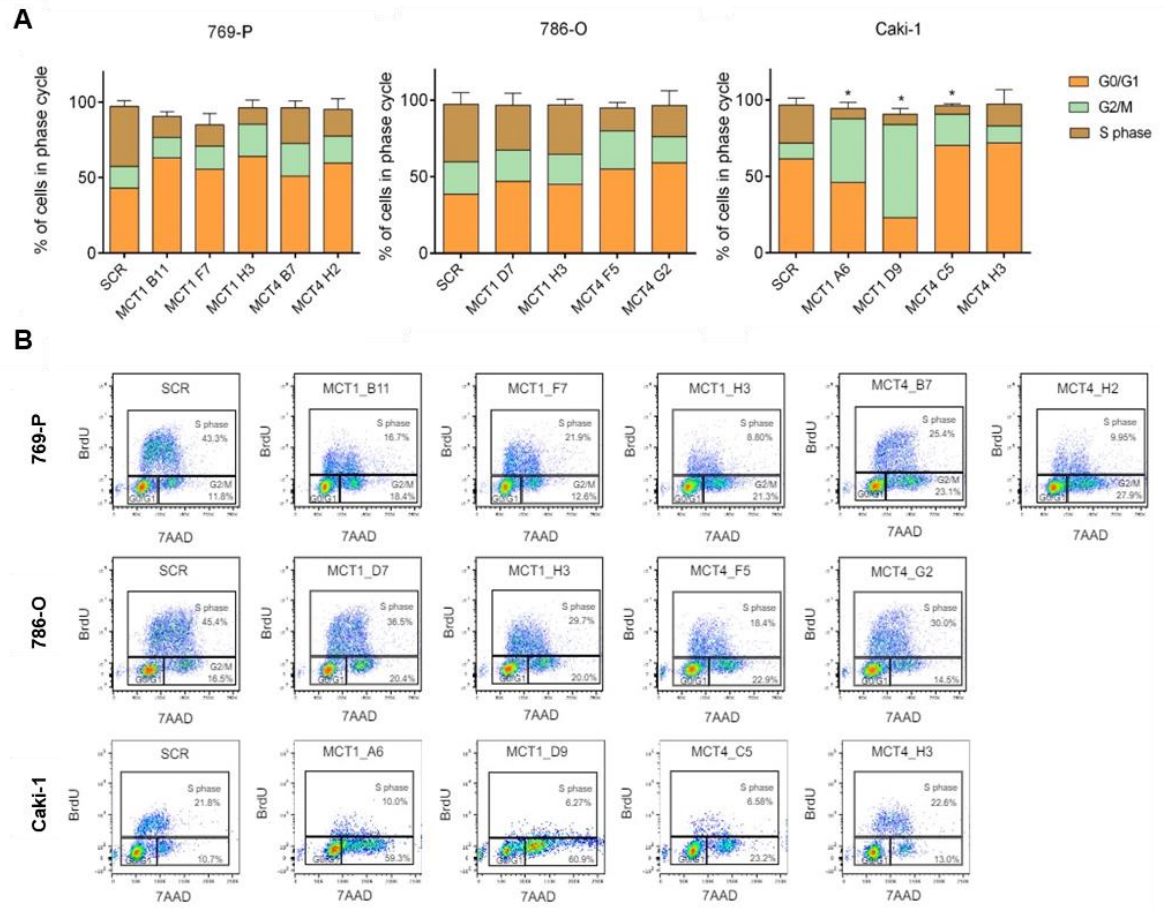

Figure 20. MCTs knockdown decreased cell proliferation in ccRCC. Graphical representation of MCTs knockdown effect in cell proliferation by BrdU incorporation assay through flow cytometry **(A)**. Representative dot-plots of 769-P, 786-O and Caki-1 cells **(B)** pulsed with 5µg/mL BrdU and then stained with Phase-Flow™ BrdU Cell Proliferation kit. Results are the mean of, at least, three independent experiments. *p<0.05 for specific MCTs knockdown clone compared to scramble.

5.7. MCTs inhibition' contributed to a less aggressive phenotype in ccRCC cells

Concerning MCTs impact on tumour migration, we observed that 769-P, 786-O and Caki-1 ccRCC-MCTs knockdown cells showed a diminished migration ability compared to the scramble cells (Figure 21). In fact, 769-P MCT1 clones migration levels were lower comparing to MCT4 clones. The contrary happened for 768-O and Caki-1 cells, in which MCT4 clones had lower migration capacity comparing to MCT1 deficient cells (Figure 21). These results go along with the cell invasion ones (Figure 22), where 769-P MCT1 clones presented lower invasion capacity and Caki-1 MCT4 clones exhibited significantly fewer invading cells comparing to the scramble cells. Nonetheless, 769-P MCT4 clones and 786-O MCTs knockdown cells did not show significant results regarding cell invasion (Figure 22).

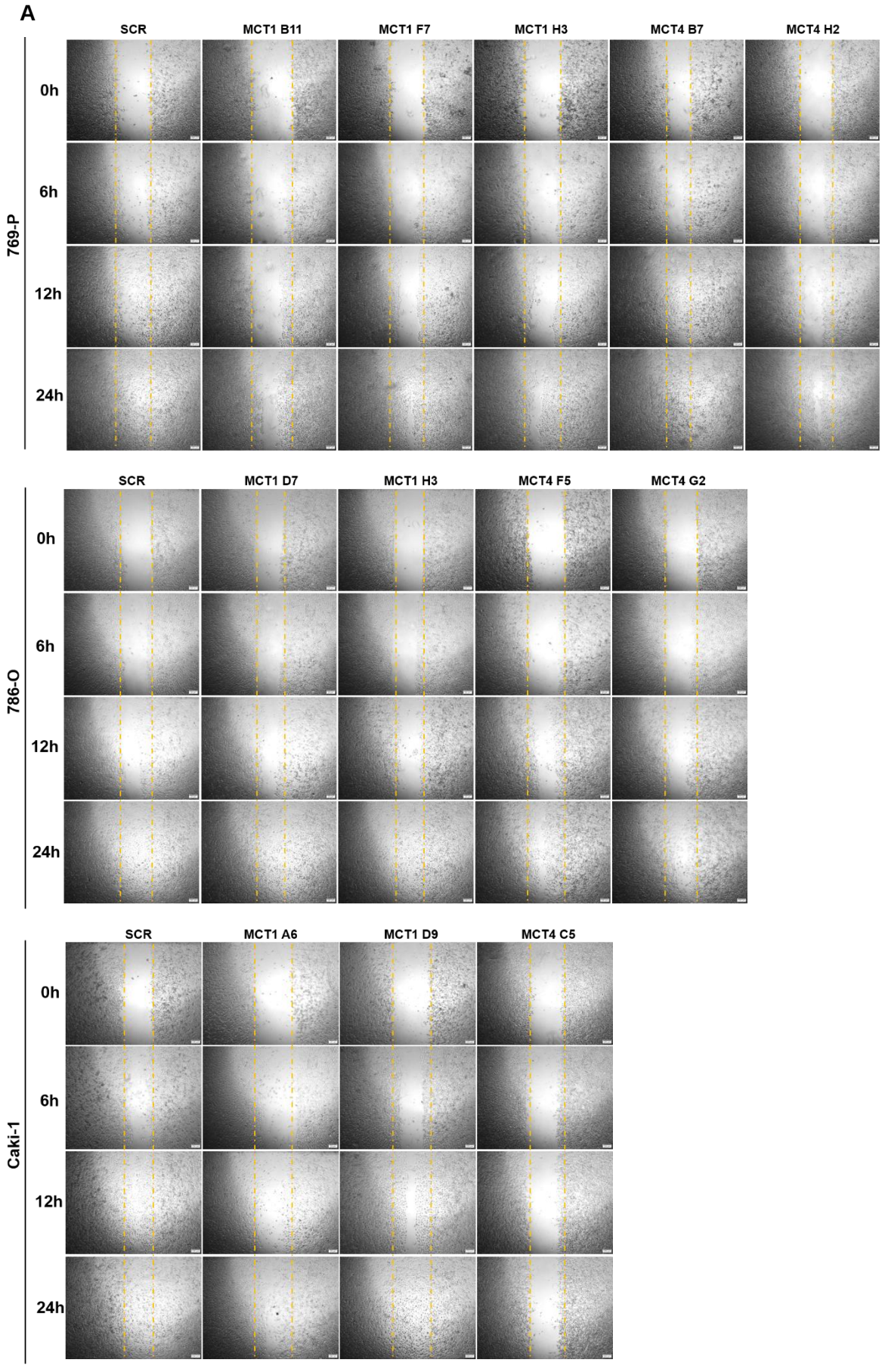
A
SCR
MCT1 B11
MCT1 F7
MCT1 H3
MCT4 B7
MCT4 H2
769-P
0h
6h
12h
24h
SCR
MCT1 D7
MCT1 H3
MCT4 F5
MCT4 G2
786-O
0h
6h
12h
24h
SCR
MCT1 A6
MCT1 D9
MCT4 C5
Caki-1
0h
6h
12h
24h

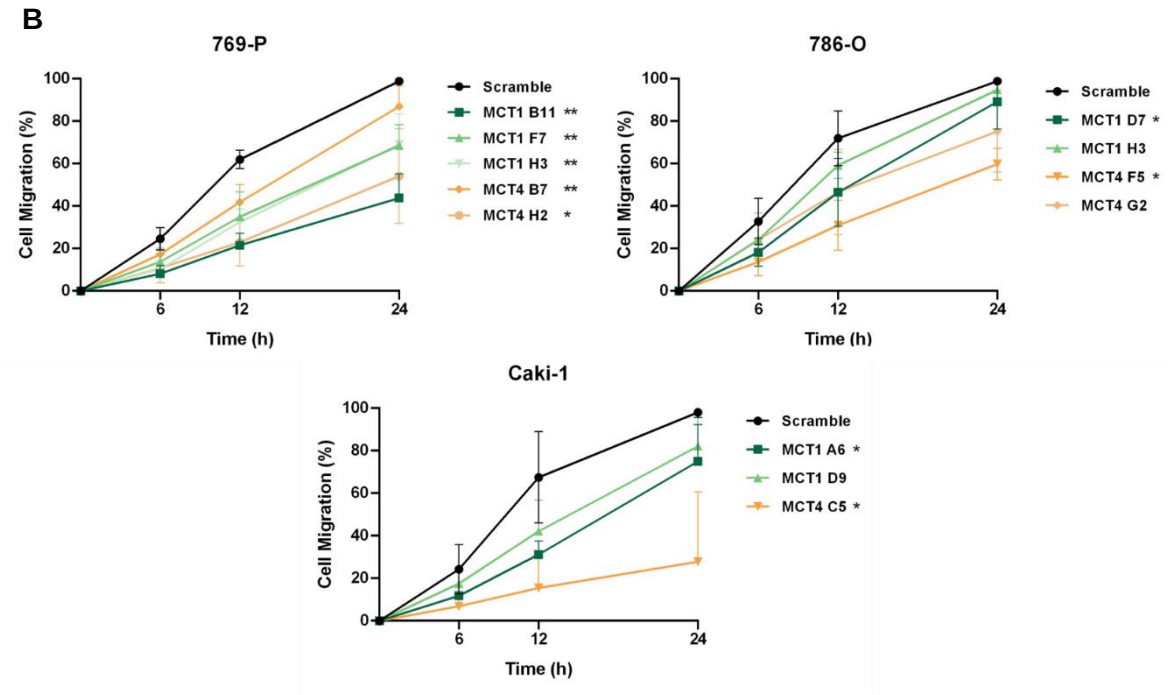

Figure 21. MCTs downregulation promoted a ccRCC cell migration decreasing. Effect of MCTs knockdown in cell migration by wound-healing assay. **(A)** Representative images of cell migration in different time points: 0h, 6h, 12h and 24h and **(B)** graphical representation of MCTs knockdown effect on cell migration capacity. Results are compared to scramble condition and are the mean of, at least, four independent experiments. *p<0.05 and **p<0.01.

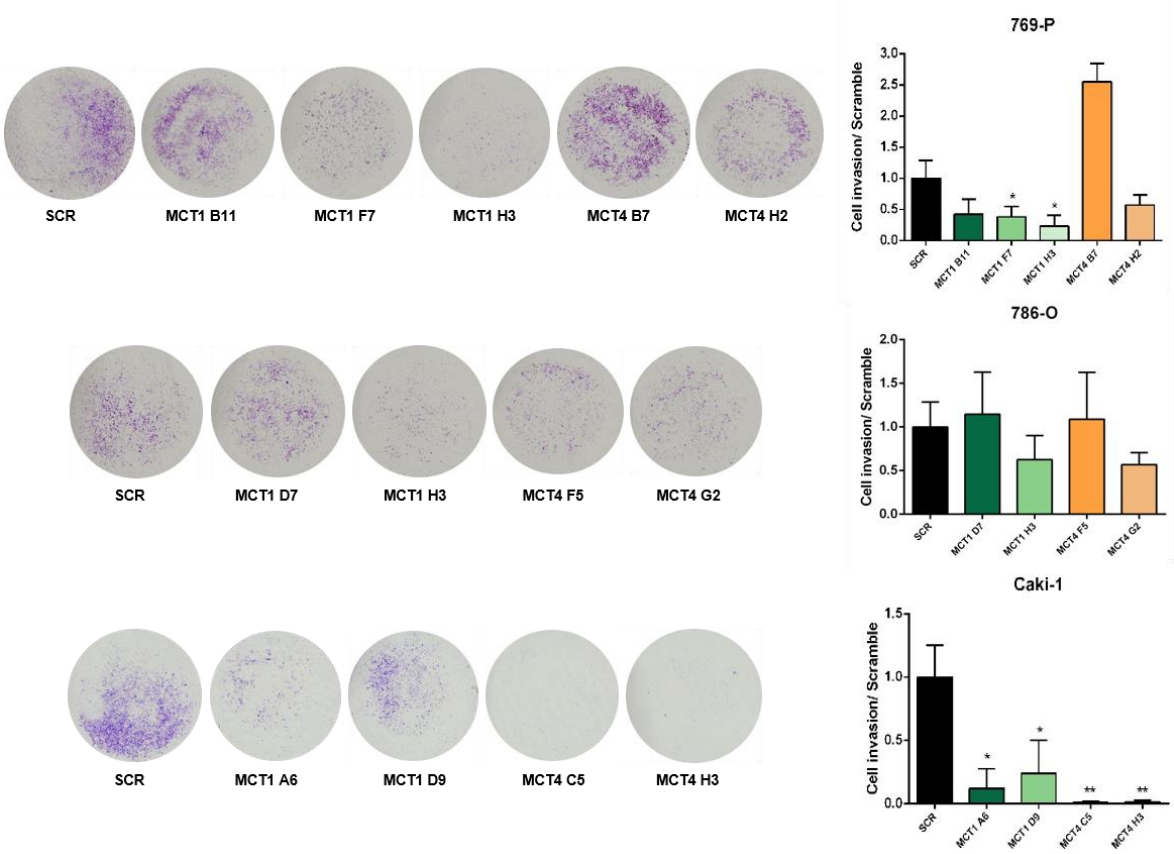

Figure 22. MCTs downregulation contributed to decreased invasion capacity in ccRCC cells. Effect of MCTs knockdown in cell invasion by BD Biosciences Matrigel Invasion Chambers assay. Results are compared to scramble condition and are the mean of, at least, four independent experiments. *p<0.05 and **p<0.01.

Finally, and because this data supports an oncogenic role of MCTs, the expression of epithelial-mesenchymal transition markers, vimentin and β–catenin, was evaluated in ccRCC-MCTs knockdown cells (Figure 23). Surprisingly, no major changes were observed in vimentin and β–catenin expression between MCT1 knockdown cells and scramble cells, except for Caki-1 MCT1 D9 clone, where a decrease in its expression could be noticed. Furthermore, a reduction in vimentin expression could be perceived in every MCT4 clone. However, β–catenin expression did not show significant changes between 786-O MCT4 clones and scramble cells. Contrarily, a downregulation in β–catenin expression was observed for 769-P and Caki-1 MCT4 clones, having been more evident in the latest.

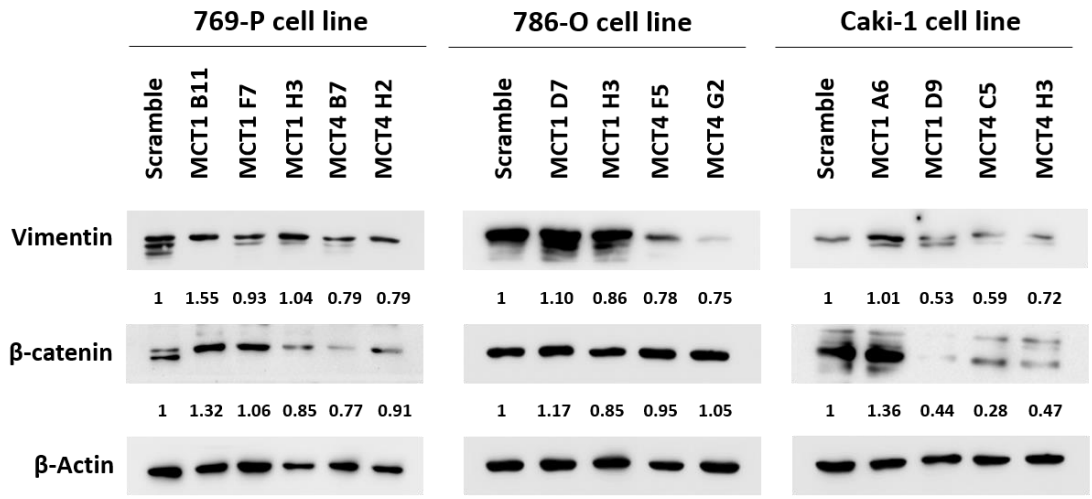

Figure 23. MCTs downregulation effect on EMT-related markers expression for ccRCC cells. The vimentin and β-catenin protein levels were assessed by WB. Results are compared to scramble condition and are the mean of, at least, four independent experiments. Molecular weights: Vimentin: 57kDa, β-catenin: 88kDa and β-actin: 42kDa.

5.8. MCTs role in *in vivo* tumour formation and progression

Using the *in vivo* CAM assay, we demonstrated that 769-P MCT1 knockdown tumours were macroscopically smaller and duller compared to scramble condition. Although no differences were depicted in tumour size between scramble cells and 769-P MCT4 knockdown cells (Figure 24A). However, a lower overall vessel recruitment was observed in 769-P MCTs knockdown clones tumours (Figure 24A). Conversely, it was not observed an evident difference in the size of 786-O MCTs knockdown tumours comparing to scramble

condition. Nonetheless, 786-O MCT4 clones presented duller tumours with lower vessel recruitment when compared to 786-O MCT1 clones and scramble condition (Figure 24B). Comparing to the scramble condition, Caki-1 MCT4 clones formed smaller tumours, and MCT4 C5 clone did not form at all, with less vessels around it (Figure 24C).

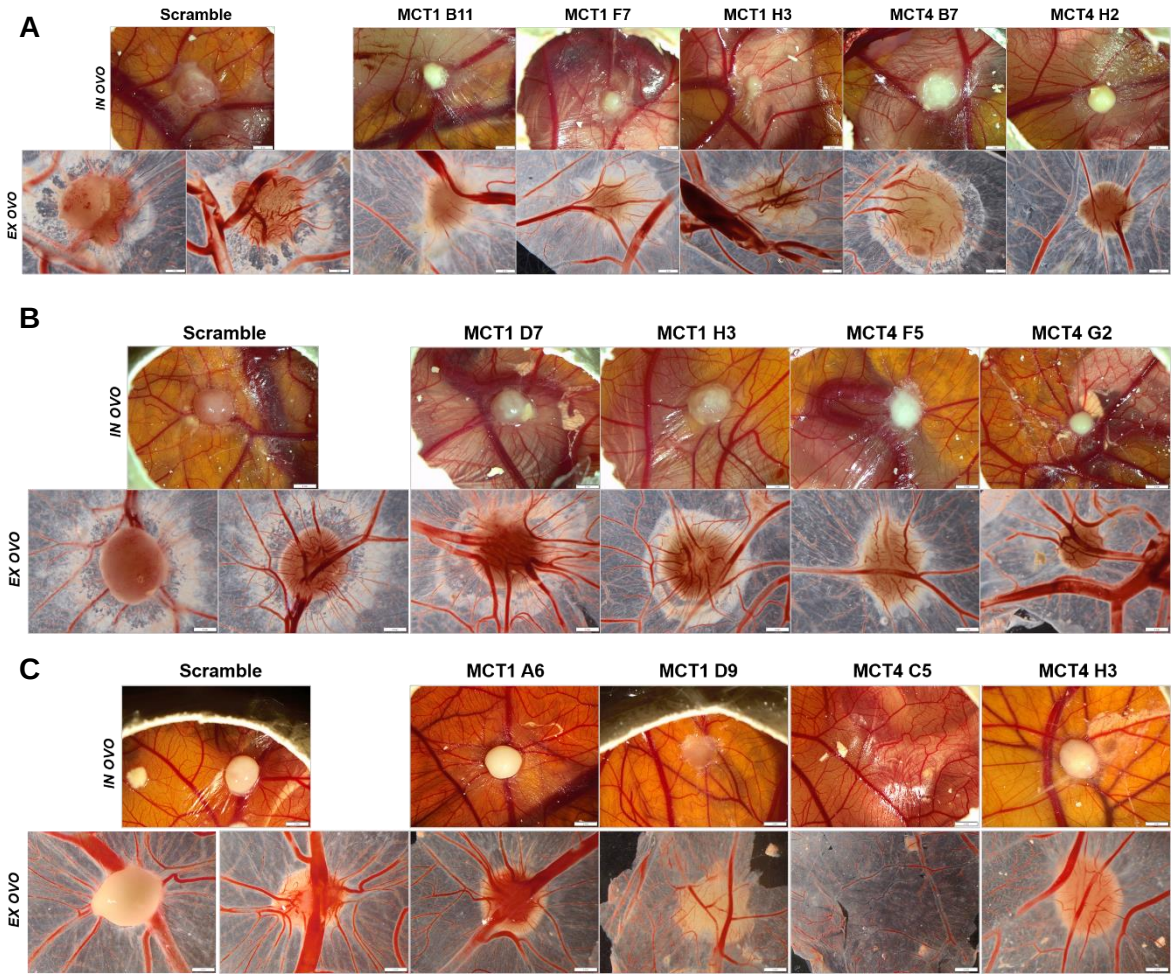

Figure 24. MCTs knockdown attenuated the in vivo ccRCC malignant phenotype. Macroscopic view of tumour formation (*in ovo* and *ex ovo*) and neo-angiogenesis in 769-P **(A),** 786-O **(B)** and Caki-1 **(C)** scramble and MCTs knockdown experimental conditions. Pictures are representative of three eggs per experimental condition.

DISCUSSION

ccRCC is the most frequent subtype of kidney cancer and, despite improvements in adjuvant therapies, the impact on survival of metastatic ccRCC patients has been limited. *VHL* is a tumour suppressor gene frequently altered in this cancer, leading to constitutive HIF activation and to a hypoxic-related metabolic reprogramming. This metabolic reprogramming induces glycolytic enzyme's upregulation and consequently an increased lactate production, which is transported through MCT1 and MCT4 to the TME, contributing to its acidification and, consequently, an increased aggressiveness and poor prognosis. Despite MCTs deregulation reported in different human cancers [55-67], few studies have described its expression in ccRCC. All these results prompted us to study the association between VHL/HIF status and the metabolic profile, specially regarding the MCTs role in ccRCC. Importantly, as pre-liminary results, our group observed a MCT1 and MCT4 upregulation in ccRCC when compared to normal kidney tissues and every case, except one, lacked VHL protein expression.

Mutational VHL inactivation is one of the earliest events in ccRCC carcinogenesis, causing HIFs constitutive activation, which induces the expression of genes that promote alterations in cellular metabolism, angiogenesis, epithelial-mesenchymal transition, tumour proliferation and metastasis formation [92]. VHL has been shown to be affected in more than 90 % of the ccRCC cases, either by allelic deletion, promoter methylation (19%), or mutations (70–80%) [93, 94]. However, there is still controversial data about the relationship between VHL mutations and pathological parameters, like the overall and disease-free survival [95, 96]. Previously in our group, an increase in promoter hypermethylation was detected in ccRCC cases when compared to normal kidney. However, since the percentage of cases in whose VHL is inactive due to epigenetic mechanisms is about 30%, we wanted to characterize our ccRCC cohort regarding the mutations that lead to *VHL* silencing. VHL p.F76del c.226_228delTTC was reported to be present in both familial and sporadic ccRCC [97]. However, only a small percentage (4%) of our ccRCC cases presented this specific mutation, highlighting the fact of further investigation needed to unveil *VHL* mutation status and its correlation with tumour progression.

HIFs are broadly expressed in human cancers and were previously suspected to promote tumour progression through overlapping functions [98]. However, this theory has been undergoing changes during the last few years and nowadays it is believed that HIF-1α and HIF-2α can promote highly divergent outcomes through regulation of different target genes [92, 98, 99]. Unlike shown in other studies [100, 101], a decrease in HIF-1α transcript levels in ccRCC when compared to normal kidney, was previously observed in our group. However, in our preliminary results HIF-1α nuclear expression was not detected in normal kidney samples but rather in ccRCC ones, confirming that HIF-1α may be regulated at post-

translational level and, in addition, its nuclear expression could predict poor survival in ccRCC, as previously described [102, 103]. Although HIF-1α was initially believed to be essential for ccRCC carcinogenesis, HIF-2α has been shown to have an important role in solid tumours development [104, 105] and has been emerging as the key player in ccRCC initiation and progression [106, 107]. Being so, we first started by determining HIF-2α expression in our cohort, having found an upregulation of this specific transcription factor in ccRCC when compared to normal kidney. On the other hand, we did not find a significant association between tumour staging and HIF-2α relative expression. In our ccRCC samples HIF-2α appears to be constitutively expressed throughout the disease development, although some studies reported as a poor prognosis marker in lung [108], colorectal [109] and gastric cancers [110-112]. Notwithstanding, some studies have shown no association between HIF-2α high expression and worse disease-specific survival in kidney cancer [113], but consider it to be important in ccRCC phenotype establishment [92], thereby supporting our data. Contrarily, a positive association between HIF-1α transcript levels and disease progression was found. Together with the high HIF-1α nuclear expression obtained for ccRCC tissues, these findings suggest that increased nuclear HIF-1α expression might be an indicator of poor prognosis for these patients, confirming the Fan, Y et al. [114] and Di Cristofano, C et.al [115] findings. Despite all the controversial data existing on HIF-1α and HIF-2α regulating tumour development and progression, our results suggest an important HIF-2α role in ccRCC initiation and phenotype maintenance, whereas HIF-1α is engaged in tumour progression and poor prognosis.

Consistent with these results, Caki-1 cell line, which represents a metastatic ccRCC, expressed slightly higher HIF-1α levels than HIF-2α. However, it should be interesting to determine HIFs differential expression in a metastatic ccRCC samples and also in ccRCC cell line with no VHL expression. According to existing data [105, 116], VHL was inactive in 769-P and 786-O cell lines, leading to HIFs stabilization and, consequently, a greater HIF-1α and HIF-2α expression observed in these ccRCC cell lines. Many HIF target-genes are described to be involved in the Warburg effect phenotype [116] and, indeed, a metabolic reprogramming was depicted by the increased protein levels of the metabolic markers GLUT, HKII, LDHA, PDK in VHL deficient cell lines, namely 769-P and 786-O cells compared to Caki-1 (VHL wildtype) cells. In fact, we observed that glucose uptake, by GLUTs, and its conversion into glucose-6-phosphate, by HKII, was higher leading to a greater lactate production by LDHA in 769-P and 786-O cells. Moreover, PDK expression was also augmented in VHL deficient ccRCC cell lines, which prevents pyruvate translocation into the mitochondria, promoting once again lactate accumulation, a common feature observed in tumour cells [117]. Thus, one can anticipate that MCTs, which are

responsible for lactate efflux, have an important role in tumour pH regulation. In fact, MCTs have been reported to be upregulated in different solid tumours and our preliminary results showed a MCT1 and MCT4 plasma membrane upregulation in ccRCC compared to normal kidney, however its role in ccRCC aggressiveness was not explored yet. Importantly, MCT1 and MCT4 protein levels were higher in 769-P and 786-O cells when compared to Caki-1 cells, suggesting that the VHL/HIFs- dependent metabolic profile was stimulating the MCTs expression and/or activity. In fact, an increased cell membrane MCT1 and MCT4 expression through an HIF-1α dependent mechanism was already described in other tumour models [51, 118]. Furthermore, Pinheiro et al. showed that GLUT1 expression was correlated with MCT1, but not MCT4, overexpression in breast tumours [119], which goes along with MCT1 higher protein levels in 786-O, also showing the highest GLUT1 and LDHA levels of the three cell lines. However, some studies reported the association of GLUT1 with MCT4, but not MCT1, in lung [120] and head and neck [121] carcinomas. Being so, the role of MCTs isoforms in the maintenance of the glycolytic phenotype may vary between tumour types.

All these results prompted us to better understand MCT1 and MCT4 roles in ccRCC carcinogenesis, from tumour growth to its aggressiveness features. Thus, we first started by evaluating glucose consumption and lactate production in MCTs-knockdown cells in the three ccRCC cell lines. Our results suggested that MCTs downregulation contributes to a reduction in ccRCC glycolytic phenotype, confirming other studies [122-124], by decreasing glucose consumption due to the diminished membrane expression of GLUT1 and cytosolic HKII and LDHA expression, mainly in 769-P MCTs knockdown cells and 786-O MCT4 knockdown clones. Furthermore, MCT4 absence seemed to have a greater impact in Caki-1 glucose metabolism, shown by the vanishing of GLUT1 and HKII expression, as well as PKM2, whose levels did not alter in 769-P and 786-O knockdown cells. Similarly to previous studies in gastric and melanoma tumour cells [125, 126], in our results MCTs-knockdown cells showed a decrease in lactate production, indicating that these proteins are also key players in mediating lactates' efflux in ccRCC. Notably, glucose consumption and lactate production levels suffered greater alterations in clones from whose MCT4 silencing percentage is greater: 786-O and Caki-1 MCT4 knockdown clones and, despite being MCT1-knockdown cells, 769-P MCT1 knockdown clones who showed only about 1% of MCT4 expression.

MCTs are important for cancer cell growth and survival [44] and a lot of effort has been invested in order to develop lactate transporters inhibitors as potential anti-tumour targets. By inhibiting MCTs in ccRCC cell lines, our results showed that all MCTs silenced cells, except 769-P MCT1 B11, decreases cell growth comparing to non-silenced cells, having this been previously reported in melanoma [126]. However, the increase in 769-P MCT1

B11 clone growth, the one that expressed higher MCT1 levels, can be explained by the increased intracellular lactate levels which inhibited PHDs promoting HIF-2α accumulation [84]. Then, HIF-2α increased glutamine uptake and catabolism through c-Myc pathway activation, sustaining tumour growth [127]. The capacity of a single MCT-knockdown cell to replicate and form a colony is lower comparing to scramble cells, without specific differences reported between MCT1 and MCT4 for 769-P and 786-O. Notably, MCT4-knockdown Caki-1 cells formed fewer colonies, pointing out the pro-tumoural advantage conferred by the expression of MCT4, already confirmed in other study [124]. Furthermore, lower proliferation levels in MCTs-knockdown cells were depicted in our work. In fact, MCTs inhibition was associated with an increased intracellular acidification and consequent reduced cell proliferation by G1 phase cell-cycle arrest in leukemia cells [128], supporting our data. MCT4, but not MCT1, was associated with increased tumour proliferation [129], supporting the fact that 769-P MCT4 B7 clone, the one expressing higher levels of MCT1 together with MCT4, revealed the smaller difference of all clones. Together, these findings suggest that combined silencing of MCT1 and MCT4 significantly reduce glycolytic flux and tumour growth.

Highly glycolytic tumours, like ccRCC are characterized by increased lactate production due to metabolic reprogramming. The excess lactate conveyed to the TME has a relevant impact in tumour biology, contributing to tumour aggressiveness features and therapy resistance [130-132]. Being so, one can predict that MCTs inhibition will attenuate tumours' aggressive behaviour. In fact, MCTs inhibition' impact on tumour migratory and invasive properties has already been shown in pancreatic cancer [133] and gliomas [55]. Despite the decrease in cell migration observed in all MCTs-knockdown cells, greater changes were noticed in the clones that expressed lower MCT4 levels: 769-P MCT1 knockdown clones, 786-O and Caki-1 MCT4 knockdown clones. Moreover, 769-P MCT4 B7 whose MCT4 expression was the highest of 769-P clones showed the highest migration rate and invasive capacities higher than the scramble cells. Interestingly, MCTs knockdown clones with lower MCT4 levels showed little or absent HIF-1α expression. Furthermore, it has been shown that lactate promotes HIF-1α accumulation in a hypoxia-independent manner in tumour cells through proline hydroxylation inhibition [36, 134]. Being so, MCT4 downregulation in ccRCC cell lines led to a decrease in the amount of lactate present in the TME and, consequently, to the depletion of HIF-1α expression. All this contributed to a less aggressive phenotype observed in MCT-knockdown cells, specially for MCT4 isoform. Accordingly, MCT4 knockdown decreased cell migration and invasion in oral squamous cell carcinoma patients [60]. Despite not having results for Caki-1 MCT4 H3 migration rates, MCT4 clones of this cell line showed the greatest decrease in cell migration and invasion. Consistently,

MCT4 has been pointed out as a poor prognostic marker in different types of human cancers [135, 136]. Adding to this, our group observed an increment in MCT4, but not in MCT1, cell membrane expression with tumour stage.

Although results of EMT-related proteins expression were not conclusive, a decrease in vimentin and β-catenin expression was observed, particularly in ccRCC cells derived from metastatic tumour (Caki-1 cells), which can be related to lactate's role on tumour progression and aggressiveness. The decreased pH potentiated by lactate oncometabolite creates the perfect environment for many of the acquired features of cancers cells, facilitating tumour immune escape and effective proteolytic degradation of the extracellular matrix by invading tumour cells [137]. A recent study showed that HIF-1α was able to induce colon cancer cells EMT [138]. Furthermore, vimentin upregulation was also observed in prostate cancer cells with HIF-1α overexpression [139]. Being so, in advanced stages of the disease, MCT4 knockdown, with consequent lactate decreased levels in the TME, leads to lower rates of tumour migration and invasion.

A partial validation of the *in vitro* findings was accomplished through the assessment of the *in vivo* tumour formation and progression. Once again, both MCT1 and MCT4 have shown to influence tumour growth as its downregulation led to smaller 769-P, 786-O and Caki-1 microtumours formation, which was equally observed in pancreatic ductal adenocarcinomas [133]. In addition, a lower vessel recruitment was prominent in clones with less MCT4 expression, confirming studies that highlight the importance of this specific MCT isoform in tumour progression and metastasis formation [135, 140].

CONCLUSIONS

Our work showed that indeed VHL inactivation, whether through promoter hypermethylation or mutation, is crucial in ccRCC carcinogenesis leading to the metabolic genes' transcription, triggered by HIF-1α and HIF-2α accumulation. Furthermore, we showed that HIF-2α was constitutively active in our ccRCC cases, being important for the phenotype establishment and maintenance, whilst HIF-1α is involved in tumour progression and related to poor prognosis. Besides, we demonstrated a perfect axis between VHL, HIFs, metabolic reprogramming and MCTs expression where HIFs' accumulation promoted by VHL absence promotes a glycolytic phenotype and consequently leads to MCTs upregulation (Figure 25).

Herein, both MCT1 and MCT4 revealed to be important in localized disease through the maintenance of high glycolytic rates allowing tumour growth and proliferation. Nonetheless, MCT4 seems to be a key player in sustaining the aggressive phenotype, since lactate increment in the TME favours tumour evasion and metastasis formation, suggesting that different MCTs should be targeted across ccRCC disease progression (Figure 25).

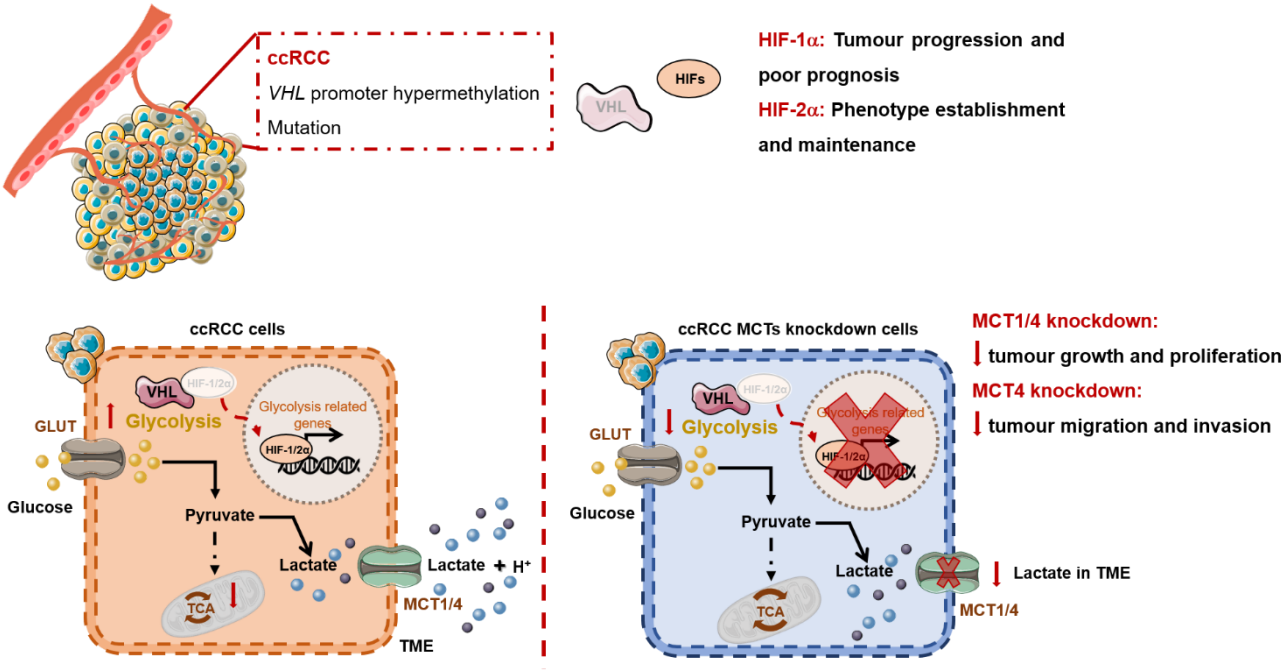

Figure 25. VHL/HIF- metabolic reprogramming and MCTs expression in ccRCC. VHL absence due to promoter hypermethylation or mutation leads to HIF-1α and HIF-2α accumulation, which promotes glycolysis related genes' transcription. This favours excessive lactate production in ccRCC cells. MCTs knockdown reduces the amount of lactate present in the TME and, consequently, ccRCC cells present lower glycolysic rates which leads to a decrease in tumour growth and proliferation. MCT4 revealed to be a crucial player in sustaining the aggressive phenotype since its knockdown led to reduced tumour migration and invasion. Abbreviations: ccRCC- clear cell renal cell carcinoma; GLUT- glucose transporter; VHL- Von Hippel Lindau; HIF- hypoxia inducible factor; TCA- tricarboxylic acid cycle; MCT- monocarboxylate transporter; TME- tumour microenvironment.

Considering our findings, tumour metabolism, particularly MCTs, was unveiled as a putative therapeutic target in ccRCC, deserving further exploration. Indeed, the use of MCTs inhibitors should be explored, as a combined treatment regime together with currently standard therapies to improve ccRCC patients' outcome.

FUTURE PERSPECTIVES

Despite the findings of the present work, many questions remain unanswered, thus, additional experiments need to be carried out in the future to complement this work.

To complement the obtained results, the identification and confirmation of VHL mosaic mutations in our ccRCC cohort is of great value to improve patient's care and provide genetic counselling to the family, since these mutations can be transmitted to the offspring. Furthermore, correlating specific *VHL* mutations with specific forms and stages of the disease, or even with specific MCTs expression, could lead to a more tailored treatment.

Moreover, it would be important to complete the *in vivo* studies to better evaluate MCTs knockdown effect in tumour size and angiogenesis, as well as characterizing metabolic and EMT markers in the obtained tumours by IHC. Finally, additional *in vitro* and *in vivo* studies for MCTs activity inhibition, with MCT1 and MCT4 specific inhibitors would be relevant to support these results.

REFERENCES

1. Padala, S.A., et al., *Epidemiology of Renal Cell Carcinoma.* World J Oncol, 2020. **11**(3): p. 79-87.
2. Hsieh, J.J., et al., *Renal cell carcinoma.* Nat Rev Dis Primers, 2017. **3**: p. 17009.
3. Escudier, B., et al., *Renal cell carcinoma: ESMO Clinical Practice Guidelines for diagnosis, treatment and follow-up†.* Ann Oncol, 2019. **30**(5): p. 706-720.
4. Sacco, E., et al., *Paraneoplastic syndromes in patients with urological malignancies.* Urol Int, 2009. **83**(1): p. 1-11.
5. Sunela, K.L., et al., *Prognostic factors and long-term survival in renal cell cancer patients.* Scand J Urol Nephrol, 2009. **43**(6): p. 454-60.
6. Ljungberg, B., et al., *European Association of Urology Guidelines on Renal Cell Carcinoma: The 2022 Update.* Eur Urol, 2022.
7. Atkins, M.B. and N.M. Tannir, *Current and emerging therapies for first-line treatment of metastatic clear cell renal cell carcinoma.* Cancer Treat Rev, 2018. **70**: p. 127-137.
8. Karami, S., et al., *Family history of cancer and renal cell cancer risk in Caucasians and African Americans.* Br J Cancer, 2010. **102**(11): p. 1676-80.
9. Schödel, J., et al., *Hypoxia, Hypoxia-inducible Transcription Factors, and Renal Cancer.* Eur Urol, 2016. **69**(4): p. 646-657.
10. Kaelin, W.G., *Von Hippel-Lindau disease.* Annu Rev Pathol, 2007. **2**: p. 145-73.
11. Ricketts, C.J., et al., *The Cancer Genome Atlas Comprehensive Molecular Characterization of Renal Cell Carcinoma.* Cell Rep, 2018. **23**(1): p. 313-326.e5.
12. Moch, H., et al., *The 2016 WHO Classification of Tumours of the Urinary System and Male Genital Organs—Part A: Renal, Penile, and Testicular Tumours.* European Urology, 2016. **70**(1): p. 93-105.
13. Inamura, K., *Renal Cell Tumors: Understanding Their Molecular Pathological Epidemiology and the 2016 WHO Classification.* International journal of molecular sciences, 2017. **18**(10): p. 2195.
14. Giles, R.H., et al., *Recommendations for the Management of Rare Kidney Cancers.* Eur Urol, 2017. **72**(6): p. 974-983.
15. Moch, H., *An overview of renal cell cancer: pathology and genetics.* Semin Cancer Biol, 2013. **23**(1): p. 3-9.
16. Haas, N.B. and K.L. Nathanson, *Hereditary kidney cancer syndromes.* Adv Chronic Kidney Dis, 2014. **21**(1): p. 81-90.
17. Banks, R.E., et al., *Genetic and epigenetic analysis of von Hippel-Lindau (VHL) gene alterations and relationship with clinical variables in sporadic renal cancer.* Cancer Res, 2006. **66**(4): p. 2000-11.
18. Dupont, C., D.R. Armant, and C.A. Brenner, *Epigenetics: definition, mechanisms and clinical perspective.* Seminars in reproductive medicine, 2009. **27**(5): p. 351-357.
19. Sharma, S., T.K. Kelly, and P.A. Jones, *Epigenetics in cancer.* Carcinogenesis, 2010. **31**(1): p. 27-36.
20. Paluch, B.E., et al., *Epigenetics: A primer for clinicians.* Blood reviews, 2016. **30**(4): p. 285-295.
21. Miranda-Gonçalves, V., et al., *Metabolism and Epigenetic Interplay in Cancer: Regulation and Putative Therapeutic Targets.* Frontiers in Genetics, 2018. **9**(427).
22. Miranda-Gonçalves, V., et al., *Metabolism and Epigenetic Interplay in Cancer: Regulation and Putative Therapeutic Targets.* Frontiers in genetics, 2018. **9**: p. 427-427.
23. Portela, A. and M. Esteller, *Epigenetic modifications and human disease.* Nature Biotechnology, 2010. **28**(10): p. 1057-1068.
24. Joosten, S.C., et al., *Epigenetics in renal cell cancer: mechanisms and clinical applications.* Nat Rev Urol, 2018. **15**(7): p. 430-451.

25. Lasseigne, B.N. and J.D. Brooks, *The Role of DNA Methylation in Renal Cell Carcinoma.* Molecular diagnosis & therapy, 2018. **22**(4): p. 431-442.
26. Liberti, M.V. and J.W. Locasale, *The Warburg Effect: How Does it Benefit Cancer Cells?* Trends Biochem Sci, 2016. **41**(3): p. 211-218.
27. Miranda-Gonçalves, V., et al., *The metabolic landscape of urological cancers: New therapeutic perspectives.* Cancer Lett, 2020. **477**: p. 76-87.
28. Stine, Z.E., et al., *Targeting cancer metabolism in the era of precision oncology.* Nat Rev Drug Discov, 2022. **21**(2): p. 141-162.
29. Yoo, A., et al., *Genomic and Metabolic Hallmarks of SDH- and FH-deficient Renal Cell Carcinomas.* European Urology Focus, 2022.
30. van der Mijn, J.C., et al., *Novel drugs that target the metabolic reprogramming in renal cell cancer.* Cancer & Metabolism, 2016. **4**(1): p. 14.
31. Sanders, E. and S. Diehl, *Analysis and interpretation of transcriptomic data obtained from extended Warburg effect genes in patients with clear cell renal cell carcinoma.* Oncoscience, 2015. **2**(2): p. 151-86.
32. Pinthus, J.H., et al., *Metabolic features of clear-cell renal cell carcinoma: mechanisms and clinical implications.* Canadian Urological Association journal = Journal de l'Association des urologues du Canada, 2011. **5**(4): p. 274-282.
33. Horiguchi, A., et al., *Fatty acid synthase over expression is an indicator of tumor aggressiveness and poor prognosis in renal cell carcinoma.* J Urol, 2008. **180**(3): p. 1137-40.
34. Shroff, E.H., et al., *MYC oncogene overexpression drives renal cell carcinoma in a mouse model through glutamine metabolism.* Proc Natl Acad Sci U S A, 2015. **112**(21): p. 6539-44.
35. Maxwell, P.H., et al., *The tumour suppressor protein VHL targets hypoxia-inducible factors for oxygen-dependent proteolysis.* Nature, 1999. **399**(6733): p. 271-275.
36. Lu, H., R.A. Forbes, and A. Verma, *Hypoxia-inducible factor 1 activation by aerobic glycolysis implicates the Warburg effect in carcinogenesis.* J Biol Chem, 2002. **277**(26): p. 23111-5.
37. Cassavaugh, J. and K.M. Lounsbury, *Hypoxia-mediated biological control.* J Cell Biochem, 2011. **112**(3): p. 735-44.
38. Lameirinhas, A., et al., *The Complex Interplay between Metabolic Reprogramming and Epigenetic Alterations in Renal Cell Carcinoma.* Genes, 2019. **10**(4): p. 264.
39. Soltysova, A., et al., *Deregulation of energetic metabolism in the clear cell renal cell carcinoma: A multiple pathway analysis based on microarray profiling.* Int J Oncol, 2015. **47**(1): p. 287-295.
40. Miranda-Gonçalves, V., et al., *The metabolic landscape of urological cancers: New therapeutic perspectives.* Cancer Letters, 2020. **477**: p. 76-87.
41. Brahimi-Horn, M.C., G. Bellot, and J. Pouysségur, *Hypoxia and energetic tumour metabolism.* Current opinion in genetics & development, 2010. **21**: p. 67-72.
42. Bacigalupa, Z.A. and W.K. Rathmell, *Beyond glycolysis: Hypoxia signaling as a master regulator of alternative metabolic pathways and the implications in clear cell renal cell carcinoma.* Cancer letters, 2020. **489**: p. 19-28.
43. Payen, V.L., et al., *Monocarboxylate transporters in cancer.* Mol Metab, 2020. **33**: p. 48-66.
44. Sun, X., et al., *Role of Proton-Coupled Monocarboxylate Transporters in Cancer: From Metabolic Crosstalk to Therapeutic Potential.* Front Cell Dev Biol, 2020. **8**: p. 651.
45. Halestrap, A.P. and N.T. Price, *The proton-linked monocarboxylate transporter (MCT) family: structure, function and regulation.* The Biochemical journal, 1999. **343 Pt 2**(Pt 2): p. 281-299.
46. Pérez-Escuredo, J., et al., *Monocarboxylate transporters in the brain and in cancer.* Biochim Biophys Acta, 2016. **1863**(10): p. 2481-97.
47. Halestrap, A.P., *The monocarboxylate transporter family—Structure and functional characterization.* IUBMB Life, 2012. **64**(1): p. 1-9.
48. Merezhinskaya, N. and W.N. Fishbein, *Monocarboxylate transporters: past, present, and future.* Histol Histopathol, 2009. **24**(2): p. 243-64.

49. Felmlee, M.A., et al., *Monocarboxylate Transporters (SLC16): Function, Regulation, and Role in Health and Disease.* Pharmacol Rev, 2020. **72**(2): p. 466-485.
50. Pinheiro, C., et al., *Monocarboxylate Transporters 1 and 4 Are Associated with CD147 in Cervical Carcinoma.* Disease Markers, 2009. **26**: p. 169678.
51. Miranda-Gonçalves, V., et al., *Hypoxia-mediated upregulation of MCT1 expression supports the glycolytic phenotype of glioblastomas.* Oncotarget, 2016. **7**(29).
52. Afonso, J., et al., *CD147 and MCT1-potential partners in bladder cancer aggressiveness and cisplatin resistance.* Mol Carcinog, 2015. **54**(11): p. 1451-66.
53. Halestrap, A.P. and D. Meredith, *The SLC16 gene family-from monocarboxylate transporters (MCTs) to aromatic amino acid transporters and beyond.* Pflugers Arch, 2004. **447**(5): p. 619-28.
54. Dimmer, K.S., et al., *The low-affinity monocarboxylate transporter MCT4 is adapted to the export of lactate in highly glycolytic cells.* Biochem J, 2000. **350 Pt 1**(Pt 1): p. 219-27.
55. Miranda-Gonçalves, V., et al., *Monocarboxylate transporters (MCTs) in gliomas: expression and exploitation as therapeutic targets.* Neuro Oncol, 2013. **15**(2): p. 172-88.
56. Choi, J.W., et al., *Prognostic significance of lactate/proton symporters MCT1, MCT4, and their chaperone CD147 expressions in urothelial carcinoma of the bladder.* Urology, 2014. **84**(1): p. 245.e9-15.
57. Pinheiro, C., et al., *The prognostic value of CD147/EMMPRIN is associated with monocarboxylate transporter 1 co-expression in gastric cancer.* European Journal of Cancer, 2009. **45**(13): p. 2418-2424.
58. Lee, J.Y., et al., *MCT4 as a potential therapeutic target for metastatic gastric cancer with peritoneal carcinomatosis.* Oncotarget, 2016. **7**(28).
59. Huhta, H., et al., *Intratumoral lactate metabolism in Barrett's esophagus and adenocarcinoma.* Oncotarget, 2017. **8**(14).
60. Zhu, J., et al., *Monocarboxylate Transporter 4 Facilitates Cell Proliferation and Migration and Is Associated with Poor Prognosis in Oral Squamous Cell Carcinoma Patients.* PLOS ONE, 2014. **9**(1): p. e87904.
61. Hao, J., et al., *Co-expression of CD147 (EMMPRIN), CD44v3-10, MDR1 and monocarboxylate transporters is associated with prostate cancer drug resistance and progression.* British Journal of Cancer, 2010. **103**(7): p. 1008-1018.
62. Doyen, J., et al., *Expression of the hypoxia-inducible monocarboxylate transporter MCT4 is increased in triple negative breast cancer and correlates independently with clinical outcome.* Biochemical and Biophysical Research Communications, 2014. **451**(1): p. 54-61.
63. Pinheiro, C., et al., *Increasing expression of monocarboxylate transporters 1 and 4 along progression to invasive cervical carcinoma.* International journal of gynecological pathology : official journal of the International Society of Gynecological Pathologists, 2008. **27**(4): p. 568-574.
64. Chen, H., et al., *Co-expression of CD147/EMMPRIN with monocarboxylate transporters and multiple drug resistance proteins is associated with epithelial ovarian cancer progression.* Clinical & Experimental Metastasis, 2010. **27**(8): p. 557-569.
65. Nakayama, Y., et al., *Prognostic significance of monocarboxylate transporter 4 expression in patients with colorectal cancer.* Exp Ther Med, 2012. **3**(1): p. 25-30.
66. Ho, J., et al., *Importance of glycolysis and oxidative phosphorylation in advanced melanoma.* Molecular Cancer, 2012. **11**(1): p. 76.
67. Pinheiro, C., et al., *The metabolic microenvironment of melanomas: Prognostic value of MCT1 and MCT4.* Cell Cycle, 2016. **15**(11): p. 1462-70.
68. Almeida, L., et al., *GLUT1, MCT1/4 and CD147 overexpression supports the metabolic reprogramming in papillary renal cell carcinoma.* Histol Histopathol, 2017. **32**(10): p. 1029-1040.
69. de Carvalho, P.A., et al., *MCT1 expression is independently related to shorter cancer-specific survival in clear cell renal cell carcinoma.* Carcinogenesis, 2021. **42**(12): p. 1420-1427.

70. Kim, Y., et al., *Expression of lactate/H⁺ symporters MCT1 and MCT4 and their chaperone CD147 predicts tumor progression in clear cell renal cell carcinoma: immunohistochemical and The Cancer Genome Atlas data analyses.* Hum Pathol, 2015. **46**(1): p. 104-12.
71. Cao, Y.W., et al., *Monocarboxylate transporters MCT1 and MCT4 are independent prognostic biomarkers for the survival of patients with clear cell renal cell carcinoma and those receiving therapy targeting angiogenesis.* Urol Oncol, 2018. **36**(6): p. 311.e15-311.e25.
72. Gerlinger, M., et al., *Genome-wide RNA interference analysis of renal carcinoma survival regulators identifies MCT4 as a Warburg effect metabolic target.* J Pathol, 2012. **227**(2): p. 146-56.
73. Fisel, P., et al., *MCT4 surpasses the prognostic relevance of the ancillary protein CD147 in clear cell renal cell carcinoma.* Oncotarget, 2015. **6**(31): p. 30615-30627.
74. Doherty, J.R. and J.L. Cleveland, *Targeting lactate metabolism for cancer therapeutics.* J Clin Invest, 2013. **123**(9): p. 3685-92.
75. Romero-Garcia, S., et al., *Lactate Contribution to the Tumor Microenvironment: Mechanisms, Effects on Immune Cells and Therapeutic Relevance.* Frontiers in Immunology, 2016. **7**(52).
76. de la Cruz-López, K.G., et al., *Lactate in the Regulation of Tumor Microenvironment and Therapeutic Approaches.* Frontiers in Oncology, 2019. **9**(1143).
77. Liu, M., et al., *Epithelial-mesenchymal transition induction is associated with augmented glucose uptake and lactate production in pancreatic ductal adenocarcinoma.* Cancer Metab, 2016. **4**: p. 19.
78. Mohamed, H., et al., *Expression and Role of E-Cadherin, β-Catenin, and Vimentin in Human Papillomavirus–Positive and Human Papillomavirus–Negative Oropharyngeal Squamous Cell Carcinoma.* Journal of Histochemistry & Cytochemistry, 2020. **68**(9): p. 595-606.
79. Sonveaux, P., et al., *Targeting the Lactate Transporter MCT1 in Endothelial Cells Inhibits Lactate-Induced HIF-1 Activation and Tumor Angiogenesis.* PLOS ONE, 2012. **7**(3): p. e33418.
80. Tabatabaei, P., et al., *Glucose metabolites, glutamate and glycerol in malignant glioma tumours during radiotherapy.* J Neurooncol, 2008. **90**(1): p. 35-9.
81. Stone, S.C., et al., *Lactate secreted by cervical cancer cells modulates macrophage phenotype.* J Leukoc Biol, 2019. **105**(5): p. 1041-1054.
82. Thommen, D.S. and T.N. Schumacher, *T Cell Dysfunction in Cancer.* Cancer Cell, 2018. **33**(4): p. 547-562.
83. Pinheiro, C., et al., *Role of monocarboxylate transporters in human cancers: state of the art.* J Bioenerg Biomembr, 2012. **44**(1): p. 127-39.
84. Sonveaux, P., et al., *Targeting lactate-fueled respiration selectively kills hypoxic tumor cells in mice.* J Clin Invest, 2008. **118**(12): p. 3930-42.
85. Gallagher, S.M., et al., *Monocarboxylate transporter 4 regulates maturation and trafficking of CD147 to the plasma membrane in the metastatic breast cancer cell line MDA-MB-231.* Cancer Res, 2007. **67**(9): p. 4182-9.
86. Renner, K., et al., *Restricting Glycolysis Preserves T Cell Effector Functions and Augments Checkpoint Therapy.* Cell Rep, 2019. **29**(1): p. 135-150.e9.
87. Price, N.T., V.N. Jackson, and A.P. Halestrap, *Cloning and sequencing of four new mammalian monocarboxylate transporter (MCT) homologues confirms the existence of a transporter family with an ancient past.* Biochem J, 1998. **329 (Pt 2)**(Pt 2): p. 321-8.
88. Brandsma, D. and M.J. van den Bent, *Molecular targeted therapies and chemotherapy in malignant gliomas.* Curr Opin Oncol, 2007. **19**(6): p. 598-605.
89. Kim, Y., et al., *Expression of lactate/H+ symporters MCT1 and MCT4 and their chaperone CD147 predicts tumor progression in clear cell renal cell carcinoma: immunohistochemical and The Cancer Genome Atlas data analyses.* Human Pathology, 2015. **46**(1): p. 104-112.

90. Brodaczewska, K.K., et al., *Choosing the right cell line for renal cell cancer research.* Molecular Cancer, 2016. **15**(1): p. 83.
91. Biswas, S., et al., *Effects of HIF-1alpha and HIF2alpha on Growth and Metabolism of Clear-Cell Renal Cell Carcinoma 786-0 Xenografts.* Journal of oncology, 2010. **2010**: p. 757908-757908.
92. Hoefflin, R., et al., *HIF-1α and HIF-2α differently regulate tumour development and inflammation of clear cell renal cell carcinoma in mice.* Nat Commun, 2020. **11**(1): p. 4111.
93. Gossage, L. and T. Eisen, *Alterations in VHL as potential biomarkers in renal-cell carcinoma.* Nat Rev Clin Oncol, 2010. **7**(5): p. 277-88.
94. Young, A.C., et al., *Analysis of VHL Gene Alterations and their Relationship to Clinical Parameters in Sporadic Conventional Renal Cell Carcinoma.* Clin Cancer Res, 2009. **15**(24): p. 7582-7592.
95. Cowey, C.L. and W.K. Rathmell, *VHL gene mutations in renal cell carcinoma: role as a biomarker of disease outcome and drug efficacy.* Curr Oncol Rep, 2009. **11**(2): p. 94-101.
96. Schraml, P., et al., *VHL mutations and their correlation with tumour cell proliferation, microvessel density, and patient prognosis in clear cell renal cell carcinoma.* J Pathol, 2002. **196**(2): p. 186-93.
97. Maher, E.R., et al., *Phenotypic expression in von Hippel-Lindau disease: correlations with germline VHL gene mutations.* J Med Genet, 1996. **33**(4): p. 328-32.
98. Keith, B., R.S. Johnson, and M.C. Simon, *HIF1α and HIF2α: sibling rivalry in hypoxic tumour growth and progression.* Nat Rev Cancer, 2011. **12**(1): p. 9-22.
99. Szendrői, A., et al., *Opposite prognostic roles of HIF1α and HIF2α expressions in bone metastatic clear cell renal cell cancer.* Oncotarget, 2016. **7**(27): p. 42086-42098.
100. Lidgren, A., et al., *The expression of hypoxia-inducible factor 1alpha is a favorable independent prognostic factor in renal cell carcinoma.* Clin Cancer Res, 2005. **11**(3): p. 1129-35.
101. Wiesener, M.S., et al., *Constitutive activation of hypoxia-inducible genes related to overexpression of hypoxia-inducible factor-1alpha in clear cell renal carcinomas.* Cancer Res, 2001. **61**(13): p. 5215-22.
102. Shenoy, N., *HIF1α is not a target of 14q deletion in clear cell renal cancer.* Scientific Reports, 2020. **10**(1): p. 17642.
103. Minardi, D., et al., *Survival in patients with clear cell renal cell carcinoma is predicted by HIF-1α expression.* Anticancer Res, 2015. **35**(1): p. 433-8.
104. Zhao, J., et al., *The role of hypoxia-inducible factor-2 in digestive system cancers.* Cell Death & Disease, 2015. **6**(1): p. e1600-e1600.
105. Pavlakis, D., et al., *Hypoxia-Inducible Factor 2α Expression Is Positively Correlated With Gleason Score in Prostate Cancer.* Technology in Cancer Research & Treatment, 2021. **20**: p. 1533033821990010.
106. Choi, W.S.W., J. Boland, and J. Lin, *Hypoxia-Inducible Factor-2α as a Novel Target in Renal Cell Carcinoma.* Journal of kidney cancer and VHL, 2021. **8**(2): p. 1-7.
107. Arnaiz, E., et al., *Differential effects of HIF2α antagonist and HIF2α silencing in renal cancer and sensitivity to repurposed drugs.* BMC Cancer, 2021. **21**(1): p. 896.
108. Higashi, K., et al., *Correlation of HIF-1α/HIF-2α expression with FDG uptake in lung adenocarcinoma.* Ann Nucl Med, 2016. **30**(10): p. 708-715.
109. Yoshimura, H., et al., *Prognostic impact of hypoxia-inducible factors 1alpha and 2alpha in colorectal cancer patients: correlation with tumor angiogenesis and cyclooxygenase-2 expression.* Clin Cancer Res, 2004. **10**(24): p. 8554-60.
110. Gao, Z.-J., et al., *HIF-2α not HIF-1α overexpression confers poor prognosis in non–small cell lung cancer.* Tumor Biology, 2017. **39**(6): p. 1010428317709637.
111. Helczynska, K., et al., *Hypoxia-Inducible Factor-2α Correlates to Distant Recurrence and Poor Outcome in Invasive Breast Cancer.* Cancer Research, 2008. **68**(22): p. 9212-9220.

112. Tong, W.-W., et al., *HIF2α is associated with poor prognosis and affects the expression levels of survivin and cyclin D1 in gastric carcinoma.* Int J Oncol, 2015. **46**(1): p. 233-242.
113. Moreno Roig, E., et al., *Prognostic Role of Hypoxia-Inducible Factor-2α Tumor Cell Expression in Cancer Patients: A Meta-Analysis.* Frontiers in Oncology, 2018. **8**.
114. Fan, Y., et al., *Prognostic Significance of Hypoxia-Inducible Factor Expression in Renal Cell Carcinoma: A PRISMA-compliant Systematic Review and Meta-Analysis.* Medicine (Baltimore), 2015. **94**(38): p. e1646.
115. Di Cristofano, C., et al., *Nuclear expression of hypoxia-inducible factor-1alpha in clear cell renal cell carcinoma is involved in tumor progression.* The American journal of surgical pathology, 2007. **31**(12): p. 1875-1881.
116. Gudas, L.J., et al., *The role of HIF1α in renal cell carcinoma tumorigenesis.* J Mol Med (Berl), 2014. **92**(8): p. 825-36.
117. San-Millán, I. and G.A. Brooks, *Reexamining cancer metabolism: lactate production for carcinogenesis could be the purpose and explanation of the Warburg Effect.* Carcinogenesis, 2017. **38**(2): p. 119-133.
118. Ullah, M.S., A.J. Davies, and A.P. Halestrap, *The plasma membrane lactate transporter MCT4, but not MCT1, is up-regulated by hypoxia through a HIF-1alpha-dependent mechanism.* J Biol Chem, 2006. **281**(14): p. 9030-7.
119. Pinheiro, C., et al., *GLUT1 and CAIX expression profiles in breast cancer correlate with adverse prognostic factors and MCT1 overexpression.* Histol Histopathol, 2011. **26**(10): p. 1279-86.
120. Meijer, T.W., et al., *Differences in metabolism between adeno- and squamous cell non-small cell lung carcinomas: spatial distribution and prognostic value of GLUT1 and MCT4.* Lung Cancer, 2012. **76**(3): p. 316-23.
121. Rademakers, S.E., et al., *Metabolic markers in relation to hypoxia; staining patterns and colocalization of pimonidazole, HIF-1α, CAIX, LDH-5, GLUT-1, MCT1 and MCT4.* BMC Cancer, 2011. **11**: p. 167.
122. Benjamin, D., et al., *Dual Inhibition of the Lactate Transporters MCT1 and MCT4 Is Synthetic Lethal with Metformin due to NAD+ Depletion in Cancer Cells.* Cell reports, 2018. **25**(11): p. 3047-3058.e4.
123. Mathupala, S.P., P. Parajuli, and A.E. Sloan, *Silencing of monocarboxylate transporters via small interfering ribonucleic acid inhibits glycolysis and induces cell death in malignant glioma: an in vitro study.* Neurosurgery, 2004. **55**(6): p. 1410-9; discussion 1419.
124. Le Floch, R., et al., *CD147 subunit of lactate/H+ symporters MCT1 and hypoxia-inducible MCT4 is critical for energetics and growth of glycolytic tumors.* Proceedings of the National Academy of Sciences of the United States of America, 2011. **108**(40): p. 16663-16668.
125. Lee, J., et al., *MCT4 as a potential therapeutic target for metastatic gastric cancer with peritoneal carcinomatosis.* Oncotarget, 2016. **7**.
126. Su, J., X. Chen, and T. Kanekura, *A CD147-targeting siRNA inhibits the proliferation, invasiveness, and VEGF production of human malignant melanoma cells by down-regulating glycolysis.* Cancer Letters, 2009. **273**(1): p. 140-147.
127. Pérez-Escuredo, J., et al., *Lactate promotes glutamine uptake and metabolism in oxidative cancer cells.* Cell cycle (Georgetown, Tex.), 2016. **15**(1): p. 72-83.
128. Pivovarova, A.I. and G.G. MacGregor, *Glucose-dependent growth arrest of leukemia cells by MCT1 inhibition: Feeding Warburg's sweet tooth and blocking acid export as an anticancer strategy.* Biomedicine & Pharmacotherapy, 2018. **98**: p. 173-179.
129. Bovenzi, C.D., et al., *Prognostic Indications of Elevated MCT4 and CD147 across Cancer Types: A Meta-Analysis.* BioMed Research International, 2015. **2015**: p. 242437.
130. Walenta, S., et al., *High lactate levels predict likelihood of metastases, tumor recurrence, and restricted patient survival in human cervical cancers.* Cancer Res, 2000. **60**(4): p. 916-21.

131. de la Cruz-López, K.G., et al., *Lactate in the Regulation of Tumor Microenvironment and Therapeutic Approaches.* Frontiers in Oncology, 2019. **9**.
132. Woo, Y.M., et al., *Inhibition of Aerobic Glycolysis Represses Akt/mTOR/HIF-1α Axis and Restores Tamoxifen Sensitivity in Antiestrogen-Resistant Breast Cancer Cells.* PLOS ONE, 2015. **10**(7): p. e0132285.
133. Schneiderhan, W., et al., *CD147 silencing inhibits lactate transport and reduces malignant potential of pancreatic cancer cells in in vivo and in vitro models.* Gut, 2009. **58**(10): p. 1391-8.
134. McDonald, P.C., S.C. Chafe, and S. Dedhar, *Overcoming Hypoxia-Mediated Tumor Progression: Combinatorial Approaches Targeting pH Regulation, Angiogenesis and Immune Dysfunction.* Frontiers in Cell and Developmental Biology, 2016. **4**.
135. Pértega-Gomes, N., et al., *Monocarboxylate transporter 4 (MCT4) and CD147 overexpression is associated with poor prognosis in prostate cancer.* BMC Cancer, 2011. **11**: p. 312.
136. Luo, F., et al., *Enhanced glycolysis, regulated by HIF-1α via MCT-4, promotes inflammation in arsenite-induced carcinogenesis.* Carcinogenesis, 2017. **38**(6): p. 615-626.
137. Huber, V., et al., *Cancer acidity: An ultimate frontier of tumor immune escape and a novel target of immunomodulation.* Seminars in Cancer Biology, 2017. **43**: p. 74-89.
138. Zhang, W., et al., *HIF-1α Promotes Epithelial-Mesenchymal Transition and Metastasis through Direct Regulation of ZEB1 in Colorectal Cancer.* PloS one, 2015. **10**(6): p. e0129603-e0129603.
139. Luo, Y., et al., *Hypoxia-inducible factor-1alpha induces the epithelial-mesenchymal transition of human prostatecancer cells.* Chin Med J (Engl), 2006. **119**(9): p. 713-8.
140. Baenke, F., et al., *Functional screening identifies MCT4 as a key regulator of breast cancer cell metabolism and survival.* The Journal of Pathology, 2015. **237**(2): p. 152-165.